Velocity-Based Stowage Policy for Semi-Automated Fulfillment Systems

by

Amy C. Liu

B.S.E. in Mechanical Engineering
University of Michigan, Ann Arbor, 2016

SUBMITTED TO THE DEPARTMENT OF MECHANICAL ENGINEERING IN PARTIAL FULFILLMENT OF THE REQUIREMENTS FOR THE DEGREE OF

MASTER OF SCIENCE IN MECHANICAL ENGINEERING
AT THE
MASSACHUSETTS INSTITUTE OF TECHNOLOGY

JUNE 2018

Signature redacted

Signature of Author: _____

Department of Mechanical Engineering
May 25, 2018

Signature redacted

Certified by: _____

Stephen C. Graves
Abraham J. Siegel Professor of Management Science
Thesis Supervisor

Signature redacted

Accepted by: _____

Professor Rohan Abeyaratne
Chairman, Committee on Graduate Students
Department of Mechanical Engineering

Velocity-based Stowage Policy for Semi-Automated Fulfillment Systems

by

Amy C. Liu

Submitted To the Department Of Mechanical Engineering
on May 25, 2018 in partial fulfillment of the
requirements for the Degree of Master Of Science in Mechanical Engineering

Abstract

Online retail fulfillment is increasingly performed by semi-automated fulfillment systems in which inventory is stored in mobile pods that are moved by robotic drives. In this thesis, we develop a model that explores the benefits of velocity-based stowage policies for semi-automated fulfillment systems. The stowage policies decide which pods to replenish with the received inventory. Specifically, we model policies that account for the velocity of the units being stowed. By stowing higher (lower) velocity units on higher (lower) velocity pods, we expect to increase the heterogeneity of the pod velocities. Greater heterogeneity in pod velocities can yield a greater reduction in pod travel distance from velocity-based storage policies for the pod. Reducing pod travel distance could decrease the number of robotic drives that are needed for the system to maintain a certain throughput rate (Yuan, 2016). We consider the random stowage policy as our base case, in which the stowage decision for each unit does not depend on the unit's velocity. In comparison, we model three types of stowage policies that use the unit velocity in the stowage decision: two-class with informed stowage, M-class with informed stowage, and two-class with random stowage. For the two-class and M-class model with informed stowage, we assume that we can classify the units based on their expected velocity, and then use this information to make the stowage decisions; we develop an approximate model from which we can characterize the impact on reducing the pod travel distance compared to that of the base case. Using simulation, we verify the accuracy of the approximate model. For the two-class with random stowage policy, we assume that the units can be categorized as being either high velocity or low velocity; however, we assume that this categorization cannot be used at stowage and that the units are stowed onto the pods randomly. We assume, though, that we can categorize each pod as being a high or low velocity pod based on the number of high velocity units stowed on the pod. We use simulation to evaluate this policy. For each of the velocity-based stowage policies, we evaluate the sensitivity on the total system travel distance per hour by varying parameters, compared to that of the base case. We also evaluate the benefits of the two-class model with random stowage from the simulation, and compare with that of the two-class model with informed stowage.

Thesis Supervisor: Stephen C. Graves
Title: Abraham J. Siegel Professor of Management Science

Acknowledgements

First and foremost, I would like to express my gratitude to my advisor Professor Stephen Graves who has supported and guided me during my time at MIT. I am gratefully indebted to Professor Graves as a student, and I am fortunate to have him as my advisor. His knowledge, experience, patience, and support have been instrumental to the completion of this thesis. Working under his supervision has been a great pleasure in my past two years at MIT.

Realizing all the supports I gain, I would also like to extend my sincere appreciation to Dr. Rong Yuan and Professor Timothy Gutowski. My research is extended from Dr. Yuan's work. I truly appreciate his knowledge and the level of detail he documented his work. I would like to thank Professor Gutowski who allows me to use his office space.

Empowered by all my friends and people I know, I become stronger and gain courage in seeking the values that I believe in. Thank you all for being part of my life.

No word can express my gratitude to my family for forever support and encouragement. Thanks my parents for always being on my side.

Lastly, I truly appreciate all the past experiences that shaped me into who I am today.

Table of Contents

Section 1. Introduction

Online retail has been rapidly growing over the past decade. Online shopping allows customers to order anytime, provides them with a variety of products and enables convenient comparison among different choices. According to the US Census Bureau, the total e-commerce sales for 2017 was $453.46 billion, which increased 16.0 % compared to $390.99 billion in 2016, whereas the total retail sales in 2017 increased only 2.9% from 2016 (Ali, 2018). The percentage of online retail sales in total retail sales has increased steadily in the US from 2.5% in 2006 to 13.0% in 2017. Facing greater demand and with pressure from rapid growth, online retailers struggle to maintain the high volumes of orders and the higher service quality expectations.

As one of the most important components of the online retail supply chain, fulfillment centers are critical for meeting customers' service quality expectation and account for about 15% of the total supply chain cost in developed countries (Handfield et al., 2013), and are considered as cost centers (Wurman et al., 2008). There has been ongoing pressure to reduce the costs. Traditional warehouses operate on a person-to-goods model, where operators stow and pick by walking to and from the storage location. These activities are usually labor intensive as the operators spend significant amounts of time traveling in the warehouse. The cost associated with order picking alone is estimated to be as much as 55% of the total warehouse operating expense (De Koster et al., 2007).

To improve operations efficiency and reduce direct labor cost, warehouses are examining opportunities in automation with emerging technology. Automated Storage and Retrieval Systems (AS/RS) have been widely implemented for automating warehouses since their introduction in 1950s An AS/RS usually consists of racks served by cranes running along the aisles between the racks. The AS/RSs are fully automated and capable of handling pallets with no operators involved. A significant amount of research has been done since the introduction of AS/RS in its field. Hausman et al. (1976), and Graves et al. (1977) were pioneers in the field of AS/RS. Their objectives were to explore optimal storage assignments by comparing different storage assignment rules. An overview of the related work in AS/RS is summarized in Gagliardi et al. (2011), and Roodbergen et al. (2009).

Our research focuses on a new type of fulfillment center, the semi-automated fulfillment system, which was pioneered by Kiva and is also known as the robotic mobile fulfillment system. The semi-automated fulfillment systems perform on a goods-to-person model, which is en-

abled by the availability of robotic technology. Specifically, semi-automated fulfillment systems have robotic drives that can transport pods, on which inventory is stored. This feature allows operators to be at stations to pick items from the pods or to stow items on the pods. After each pick or stow operation, a robotic drive stores the pod in the storage field. With reliable robotic drives, the items are selected and delivered more efficiently according to the customer's order request. Wurman et al. (2008) introduce and describe semi-automated fulfillment systems in detail. Semi-automated fulfillment systems provide many advantages compared to AS/RS. For instance, semi-automated fulfillment systems provide flexibility and expandability, while AS/RS are difficult and costly to move once installed. Bozer and Aldarondo (2018) present a simulation-based comparison between mini-loaded AS/RS and semi-automated fulfillment systems and discuss the advantages and limitation of each system.

Our research focuses on the operational process regarding the semi-automated storage system, which involves picking, stowage, and storage. This thesis specifically focuses on the stowage aspect. The details of each operational process can be found in Yuan (2016). The key operational decisions are as follows:

- *Picking Decision.* The picking decision determines from which pod to pick each unit in each order. The inventory for each stock-keeping unit (sku) is typically stored across multiple pods. Hence there can be many options for how to pick the units required for an order, which may contain multiple skus.
- *Stowage Decision.* The stowage decision determines onto which pods to store (or stow) the received inventory from vendors in the storage system. A large fulfillment center may have multiple storage zones or fields; so the first stowage decision is to decide to which zone to send each unit. At the zone level, the objective for the stowage decision is to assign the units so as to balance the picking workload, thus reducing the costs from over-assigning orders in over-loaded zones and underutilizing the under-loaded zones. At the pod level, the stowage policy determines onto which pods to store the received inventory. This level of decision is mostly dependent on the available storage space on the pods and the physical size of the received units of inventory.
- *Storage Decision.* The storage decision determines to what location in the storage field to return a pod after the pod completes a pick or stow operation. Storage policies are placed in order to minimize the total travel distance of the robotic drives.

Enright and Wurman (2011) present resource allocation challenges in the context of semi-automated fulfillment systems. A lot of research has been done in exploring queueing and utilization aspect: Nigam et al. (2014), Lamballais et al. (2017a), Lamballais et al. (2017b), and Zou et al. (2017). Merschformann et al. (2018) present a discrete event simulation to study order assignment, pod selection and pod storage assignment problems. Yuan (2016) explores velocity-based storage decisions and examines zone and pod level stowage decisions. The velocity-based storage decisions are also explored in Yuan et al. (2018a). Yuan et al. (2018b) present ideal zone level stowage policy to balance the demand.

In this thesis, we extend the work of Yuan (2016) and develop a model that explores the benefits of velocity-based stowage policies for semi-automated fulfillment systems. We aim to approach the stowage aspect with a practical heuristic. Specifically, our goal is to model policies that account for the velocity of the units. By stowing higher (lower) velocity units on higher (lower) velocity pods, we expect that we can increase the heterogeneity of the pod velocities. Yuan (2016) has characterized the benefits from velocity-based storage policies that store high-velocity pods closer to the pick and stow stations, while placing low velocity pods further away. Yuan (2016) found that greater heterogeneity in the pod velocities could yield greater reduction in pod travel distance from velocity-based storage policies for the pod. As a result, reducing pod travel distance could decrease the number of robotic drives that are needed for the system to maintain a certain throughput rate (Enright and Wurman, 2011; Yuan, 2016; Lamballais et al., 2017).

We consider random stowage policy as our base case, in which units are not stowed by their velocity. In Section 2, we model three types of velocity-based stowage policies: two-class with informed stowage, M-class with informed stowage, and two-class with random stowage. By analyzing the two-class and M-class models with informed stowage, we assume that we can categorize the units to be stowed into two or M classes, respectively. We then can use this categorization to create corresponding classes of pods; we are able to show the impact in reducing the pod travel distance compared to the base case. In Section 3, we verify the accuracy of the model with simulation results. We then evaluate the impact on the total travel distance per hour for the system by varying the percentage of items in each class for $M = 2$ & 3, and compare the results to that of the base case. We also evaluate the benefits of the two-class model with random stowage from the simulation, and compare with that of the two-class model with informed stowage.

Section 2. Model

The intent is to develop a model that would explore the benefits of velocity-based stowage policies for the semi-automated storage system. Specifically, we would like to model policies that account for the velocity of the units. By stowing higher (lower) velocity units on higher (lower) velocity pods, we expect that we can increase the heterogeneity of the pod velocities. Greater heterogeneity in the pod velocities can yield a greater reduction in pod travel distance from velocity-based storage policies for the pod.

We consider a storage system that is effectively in steady state equilibrium and that is heavily utilized. Each pod travels to a stowage station at regular intervals for replenishment after a specified number of picks. We model the behavior of a single pod, with the intent of characterizing the pod's velocity as it depends on the stowage policy. We then use this understanding of the behavior of a single pod to extrapolate to a storage system that is operating with a given throughput rate. For this extrapolation, we assume that the pods in the system operate independently. We can then develop estimates for the total pod travel distance per hour for the system, as it depends on the unit-stowage policy and on the pod-storage policy.

In this section, we first list the model assumptions and model preliminaries. We then develop the model to evaluate the effectiveness of different stowage policies. We finally provide numerical demonstrations for the analytical results.

2.1 Model Assumptions

We model a single pod that is representative of all of the pods in the storage system. We focus on stowage events, assuming that each pod will travel to a stowage station for replenishment at regular intervals and then return to the storage system. In this section, we present and discuss the model assumptions:

A.1 *Same unit size for all items and same pod size.* We assume that all items have the same unit size, and all pods have the same capacity for holding the inventory. The pod has capacity for C units, where each unit occupies the same amount of space on the pod. We think this is a reasonable assumption for our model as each pod has the same storage volume, and will typically hold several hundred units of inventory. There is variability in the item sizes across different skus. But the average size of an item on each pod is relatively constant.

A.2 *Fixed threshold for stowage replenishment.* We set a threshold, k, so that when the number of units on the pod drops to $C - k$, the pod is replenished with k units. The size of the replenishment quantity, k, is a control parameter. Effectively, we assume that after k units are picked from the pod, the pod will go to a stowage station for replenishment. This is a reasonable proxy for how stowage decisions are made. When a stowage station has material to stow, it will call pods to the station, with priority given to pods with the most available space.

A.3 *Ample supply for stowage*. We assume that when a pod goes to a stow station for replenishment that k units are available to be stowed onto the pod; in effect, there will always be sufficient units waiting to be stowed at each station.

In order to evaluate the total travel distance of robotic drives in the storage system, we make some additional assumptions:

A.4 *High space utilization.* We assume that we have the same number of storage locations and pods in the system. During operation, if the number of pods, J, is less than the number of storage locations, we would store the pods in the J closest storage locations.

A.5 *Linear travel distance*. We define d_j to be the distance from storage location j to the nearest stowage station, where we have ranked the storage locations such that $d_j \leq d_{j+1}, j = 1,2...J$ and J is the total number of storage locations, equal to the total number of pods. We assume that we can estimate the travel distance by a linear model: $d_i = \beta \times \left({}^{i}/_{J} \right), i = 1,2...J$, where is β is a constant equal to the furthest travel distance. Justification for this assumption is based on the analysis done by Yuan (2016) for representative storage fields.

A.6 *Mass balance and fixed system throughput rate.* The throughput rate for the system is the rate at which units are being picked per hour. We assume that the storage system has a target hourly throughout rate, denoted as λ_S. We assume that the storage system is effectively in a steady-state equilibrium in that the stowage rate matches the pick rate; as a result, the number of units in storage is neither increasing nor decreasing over time. We think this assumption is reasonable for any highly utilized storage system.

We will introduce additional assumptions as they become necessary for the model development.

2.2 Model Development

In this section, we discuss the modeling of the stowage operation of a storage system where we can classify units based on their velocity (or dwell time). The dwell time for a unit is how long the unit stays in the system: the dwell time is the difference between the time that the unit gets picked and the time it was stowed into the system. We use the term velocity to correspond to a demand rate for a unit; in this context, the unit velocity is the inverse of the dwell time. Our objective is to evaluate the expected total travel distance for stowage trips for different stowage policies.

Base Case

For the base case we assume that we do not classify the units to be stowed by their velocity. The system has a target throughout rate, λ_S, which is the number of units picked per hour (Assumption A.6). We assume that the target throughput rate also corresponds to the stowage rate, the number of units stowed per hour, based on Assumption A.6 of mass balance. We assume that the dwell time for each unit has an average dwell time denoted by τ, measured in hours. That is, we assume that each unit that is stowed in the system will remain in the system for τ hours, on average, until being picked.

By Assumption A.1, each pod has the capacity to hold C units. By Assumption A.2, the number of units on each pod will range between C and $C-k$. The inventory on a pod decreases as units get picked; once the number of units remaining hits $C-k$, we assume that a stowage event will occur and will bring the inventory back to C. By Assumption A.3, each pod is replenished whenever the number of units drops to $C-k$, where k is a control parameter. Thus, we approximate the average number of units stored on each pod as

$$C-k/2. \tag{1}$$

If the pick rate from the pod were constant, then Equation (1) would not be an approximation, but would be exact. However, we cannot assume that the pick rate from the pod will be constant; for instance, when the pod is full, the rate at which units are picked is likely greater than when the pod is not full.

To characterize the average pick rate for a single pod, λ_P, we apply Little's Law: $L = \lambda W$, where L is the average number of customers waiting or in process in the system, λ is the customer arrival rate, and W is the average time that a customer arrival spends in the system. Equivalently for an individual pod, L is the average number of units on the pod; W is the average dwell time for the units in the system, namely τ; and λ is the average pick rate for the pod. From Equation (1), the average number of units on a pod is $L = C - k/2$. Therefore, we can determine the average throughput rate for each pod, λ_P, from Little's Law

$$L = \lambda W \Rightarrow C - k/2 = \lambda_P \tau, \tag{2}$$

where λ_P denotes the throughput (or pick) rate for an individual pod (units per hour); by Assumption A.6, this is the rate at which units are picked from the pod, as well as the rate at which units are stowed onto the pod. Hence, we have:

$$\lambda_P = \frac{C - k/2}{\tau}. \tag{3}$$

In order for the system to meet the target throughput rate, we need to have $J \times \lambda_P = \lambda_S$ where J is the number of pods in the system; thus:

$$J = \lambda_S / \lambda_P. \tag{4}$$

The number of pods is inherently an integer; however, for our model development we will not impose this requirement so as to not complicate the development. In reality, the number of pods is on the order of 1000's, so we expect there is minimal impact from this simplification.

We now develop a model for the travel distance associated with the stowage trips. The total travel distance per hour will be the product of the number of trips per hour times the average distance per trip.

TRAVEL DISTANCE MODEL

We now develop a model for the travel distance associated with the stowage trips.

Number of trips: Each pod makes a replenishment trip to a stow station after it has had k picks. Thus, an estimate of the average time between visits to the stow station, denoted by TBV, is $TBV = k/\lambda_P$ in hours. The number of trips each pod makes per hour is the inverse:

$1/TBV = \lambda_P/k$. Therefore, the total number of trips per hour for the system, denoted as N, is given by:

$$N = J \times {}^{\lambda_P}\!/_{k} = {}^{\lambda_S}\!/_{k}. \tag{5}$$

Average distance per trip: We assume that we have storage space for J pods, and that we can estimate the travel distance by a linear model (Assumption A.5). That is, we assume

$$d_i = \beta \times \left({}^{i}\!/_{J} \right), i = 1,2...J, \tag{6}$$

where d_i is the travel distance to the i^{th} closest location, and β is a constant equal to the furthest travel distance. We assume that after a visit to a stow station, the pods will travel to the closest open storage location; in a highly utilized storage system this will effectively be a random location storage policy (Yuan, 2016). Thus, the average travel distance is approximately: $\bar{d} = \beta/2$, where β is the furthest travel distance.

Total travel distance per hour: Therefore, for the base model, we estimate the total travel distance per hour, T_B for stowage trips to be:

$$T_B = \bar{d} \times N = \frac{\beta \lambda_S}{2k}. \tag{7}$$

Two-Class Model with Informed Stowage

In this section, we develop a model of the stowage operation of a storage system for which we can classify units into two velocity-based classes.

For the two-class model, we assume that at the time of stowage we can categorize the units to be stowed into two classes, namely a high-velocity class and a low-velocity class; that is, we have some information on the dwell times for the units to be stowed. We assume that we are given the average dwell times for high and low velocity items, denoted by $\tau_1, \tau_2, \tau_1 < \tau_2$, respectively. At the time of stowage, the actual dwell time for each unit is a random variable with the given mean. We are also given p_1, which denotes the fraction of arriving units from the high-velocity class, and p_2, which denotes the fraction of arriving units from the low-velocity class, where $p_1 + p_2 = 1$. The average dwell time for all arriving units, τ, is then:

$$\tau = p_1\tau_1 + p_2\tau_2. \tag{8}$$

Furthermore, by Assumption A.6, if λ_S is the given system throughput rate (units processed per hour), then $p_1\lambda_S$ is the arrival (or throughput) rate to stowage for high-velocity units, and $p_2\lambda_S$ is the arrival or throughput rate for low-velocity units.

We designate each pod as being either a high-velocity or a low-velocity pod. For the two-class stowage policy, we assume that we can stow each high-velocity unit onto a high-velocity pod, and each low-velocity unit onto a low-velocity pod. In the equilibrium state for the system, each high-velocity pod will carry only units from the high velocity class; similarly, each low-velocity pod carries only low-velocity units. In effect, we assume that whenever a high- or low-velocity pod goes for stowage, we are able to stow *k* high or low velocity units, respectively, on-to the pod.

The average time that each unit spends on a high-(low-) velocity pod is $\tau_1(\tau_2)$. Each pod has capacity to hold *C* units (Assumption A.1) and each pod is replenished whenever the number of units drops to $C - k$, where *k* is a control parameter (Assumption A.2). Then similar to the base case, we can determine the pick rate (units per hour), or throughput rate, for each type of pod:

$$\lambda_{1P} = \frac{C - k/2}{\tau_1}, \lambda_{2P} = \frac{C - k/2}{\tau_2}, \tag{9}$$

where λ_{1p} is the pick rate for a high-velocity pod, and λ_{2p} is the pick rate for a low-velocity pod. In order for the system to meet the target throughput rate, we need to have:

$$\begin{aligned} J_1 \times \lambda_{1p} &= p_1\lambda_S, \\ J_2 \times \lambda_{2p} &= p_2\lambda_S, \end{aligned} \tag{10}$$

where J_1 is the number of high-velocity pods, and J_2 is the number of low-velocity pods; thus with Equation (9):

$$\begin{aligned} J_1 &= p_1\lambda_S \Big/ \lambda_{1p} = \frac{p_1\tau_1\lambda_s}{C - k/2}, \\ J_2 &= p_2\lambda_S \Big/ \lambda_{2p} = \frac{p_2\tau_2\lambda_s}{C - k/2}. \end{aligned} \tag{11}$$

We see from Equation (11) that:

$$J = J_1 + J_2$$
$$= \frac{(p_1\tau_1 + p_2\tau_2)\lambda_S}{C - k/2} = \frac{\tau\lambda_S}{C - k/2}. \quad (12)$$

which agrees with the base case model (Equation (4) with Equation (3)).

TRAVEL DISTANCE MODEL

We now develop a model for the travel distance associated with the stowage trips.

Number of trips: Similar to the base case, the average time between visits for the high-velocity pods is $TBV_1 = k/\lambda_{1p}$, and for the low-velocity pods is $TBV_2 = k/\lambda_{2p}$, which are both in hours. The average number of trips each pod makes per hour is the inverse: the average number of trips that an individual high-velocity pod makes is $1/TBV_1 = \lambda_{1p}/k$; the average number of trips that an individual low-velocity pod makes is $1/TBV_2 = \lambda_{2p}/k$. Thus, the average total number of trips per hour for each class is:

$$N_1 = J_1 \times \lambda_{1P}/k = p_1\lambda_S/k,$$
$$N_2 = J_2 \times \lambda_{2P}/k = p_2\lambda_S/k. \quad (13)$$

We also see that $N_1 + N_2 = N = \lambda_S / k$, agreeing with the base model (Equation (5)).

Average travel distance: Yuan (2016) simulates the ranked travel distances from storage locations to closest station with an example (shown in Figure 2.1), and observes that the ranked travel distances can be modeled by a linear function for approximation. In addition, we assume each storage location stores a pod. Thus, we assume that the storage space is divided into two zones: high-velocity pods go to zone 1, and low–velocity pods go to zone 2, where zone 1 is the J_1 closest storage locations, and zone 2 is the remaining J_2 storage locations (shown in Figure 2.2).

FIGURE 2.1 Travel Distances from Storage Locations to the Closest Stations (Yuan, 2016).

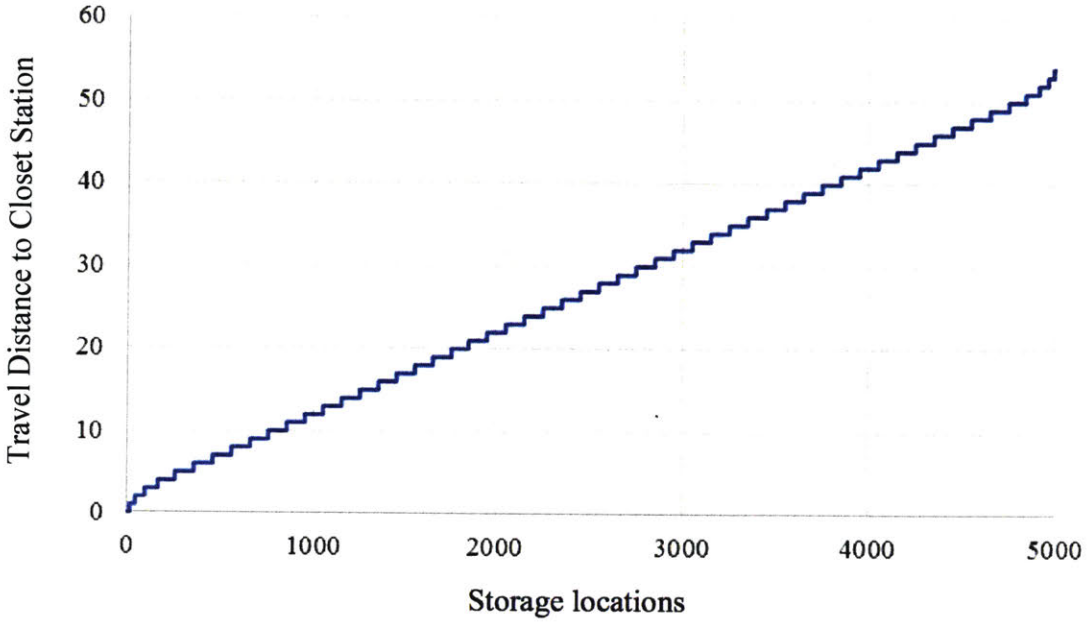

FIGURE 2.2 A linear model (Assumption A.5) for the two-class model, where β is the furthest travel distance, and J is the total number of pods in the system.

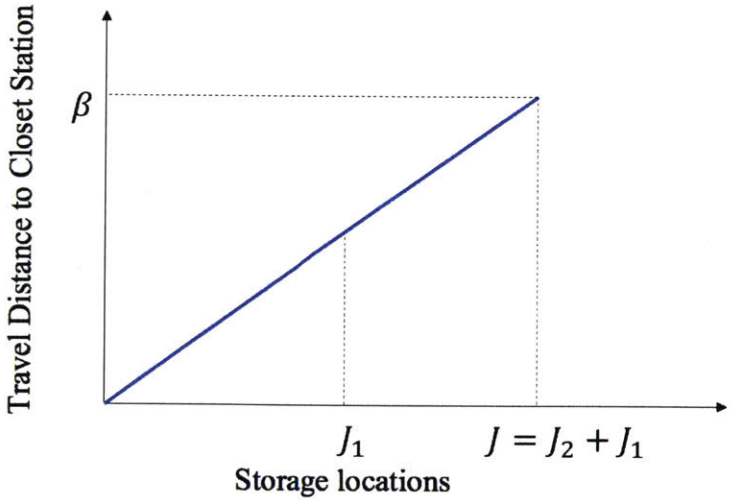

We assume that the storage within each zone is random; that is we will return a pod to any open location, with equal probability. For highly utilized systems, the assumption of random storage is a good proxy for a closest open location storage policy, as might be common in practice. With this assumption, we are able to approximate the average travel distance for each zone

by using the linear model shown in Figure 2.2 and Equation (6). As shown in Figure 2.2, the furthest travel distance for zone 1 can be approximated with $\beta J_1/J$. Therefore, the average travel distance to zone 1 can be approximated as: $\bar{d}_1 = \beta J_1/(2J)$. Also, the furthest travel distance for zone 2 can be approximated with β, and the least travel distance for zone 2 is the furthest travel distance for zone 1, $\beta J_1/J$. Therefore the average travel distance to zone 2 can be approximated as: $\bar{d}_2 = \dfrac{\beta(J+J_1)}{2J}$.

Total travel distance per hour: Therefore, the estimate for the total travel distance per hour for the two-class model is

$$\begin{aligned} T_2 &= \bar{d}_1 \times N_1 + \bar{d}_2 \times N_2 \\ &= \frac{\beta\lambda_S}{2k}\left(p_1 \frac{J_1}{J} + p_2 \frac{J+J_1}{J} \right) \\ &= \frac{\beta\lambda_S}{2k}\left(p_1 \frac{J_1}{J} + (1-p_1)\frac{J+J_1}{J} \right) \\ &= \frac{\beta\lambda_S}{2k}\left((1-p_1) + \frac{J_1}{J} \right) \\ &= \frac{\beta\lambda_S}{2k}\left((1-p_1) + p_1 \frac{\tau_1}{\tau} \right). \end{aligned} \tag{14}$$

We note that for the base case, we had $T_B = \beta\lambda_S/(2k)$; hence we see that $T_2 < T_B$ since $(1-p_1) + p_1\tau_1/\tau < 1$. Thus, the ratio of reduction in total stowage travel distance per hour for the two-class model compared to that of the base case is:

$$\frac{T_2}{T_B} = 1 - p_1 + p_1 \frac{\tau_1}{\tau}. \tag{15}$$

We illustrate the ratio of T_2/T_B in Table 1 to demonstrate how the average travel distance for the two-class model decreases relative to the base case. We can use the ratio of T_2/T_B to demonstrate the benefit in decreased travel distance from having a two-class model.

TABLE 1

Calculated Reduction in Total Travel Distance per Hour with Two-class Model.

τ	p_1	τ_1	p_2 *	τ_2 *	T_2/T_B
10.0	0.2	2.0	0.8	12.0	0.84
10.0	0.4	5.0	0.6	13.3	0.80
10.0	0.6	8.0	0.4	13.0	0.88

*With given τ, p_1, τ_1 we are also able to obtain p_2, τ_2 with $p_1 + p_2 = 1$ and Equation (8).

M-Class Model with Informed Stowage

In this section, we extend the two-class model of the stowage operation of a storage system to the case of M velocity-based classes.

For the M-class model, we assume that at the time of stowage we can categorize the units to be stowed into M classes, where class i has the i^{th} highest velocity, for $i = 1,2...M$; that is, we have some information on the average dwell times for the units to be stowed. We assume that we are given the average dwell times for items in each class, denoted by $\tau_1, \tau_2 ... \tau_M$, where $\tau_1 < \tau_2 < ... < \tau_M$. At the time of stowage, the actual dwell time for each unit is a random variable with the given mean. We are also given $p_i, i = 1,2...M$, which denotes the fraction of arriving units that are from each class i, where $\sum_{i=1}^{M} p_i = 1$. The average dwell time for all arriving units, τ, is then

$$\tau = \sum_{i=1}^{M} p_i \tau_i. \tag{16}$$

Furthermore, by Assumption A.6, if λ_S is the given system throughput rate (units processed per hour), then $p_i \lambda_S$ is the throughput rate for class i.

We assume that we are able to identify the velocity class for each incoming unit to be stowed. We designate each pod to hold units exclusively from a single velocity class. Hence we have M types of pods, one for each velocity class. We assume that we can stow each incoming unit of class i onto a corresponding pod for class i. For each class of pods, each pod has the ca-

pacity to hold C units (Assumption A.1) and each pod is replenished whenever the number of units drops to $C-k$, where k is a control parameter (Assumption A.2). Then, similar to the two-class model, we can determine the pick rate (units per hour), or throughput rate, for each type of pod:

$$\lambda_{iP} = \frac{C - k/2}{\tau_i}, i = 1,2...M, \tag{17}$$

where λ_{ip} is the pick rate for each class's pod. In order for the system to meet the target throughput rate, we need to have

$$J_i \times \lambda_{ip} = p_i \lambda_S, \tag{18}$$

where J_i is the number of pods for each class i, where $i = 1,2...M$. Thus, with Equation (17):

$$J_i = p_i \lambda_S / \lambda_{ip} = \frac{p_i \tau_i \lambda_s}{C - k/2}. \tag{19}$$

We see from Equation (19) that:

$$\begin{aligned} J &= \sum_{i=1}^{M} J_i \\ &= \frac{\sum_{i=1}^{M} p_i \tau_i \lambda_S}{C - k/2} = \frac{\tau \lambda_S}{C - k/2}, \end{aligned} \tag{20}$$

which agrees with the base case model (Equation (4) with Equation (3)).

TRAVEL DISTANCE MODEL

We now develop a model for the travel distance associated with the stowage trips.

Number of trips: Similar to the two-class model, the time between visits for the pods of class i is $TBV_i = k/\lambda_{ip}$, which is in hours. The number of trips each pod makes per hour is the inverse: the average number of trips that a pod from class i makes is $1/TBV_i = \lambda_{ip}/k$. Thus, the number of trips per hour for each class i is found to be

$$N_i = J_i \times \lambda_{iP}/k = p_i \lambda_S / k. \tag{21}$$

We see that $\sum_{i=1}^{M} N_i = N = \lambda_S / k$, agreeing with the base model (Equation(5)).

Average travel distance: Now we assume the storage space is divided into M zones, where the i^{th} highest velocity pods go to zone i. We assume that the zones are determined such that the locations in zone i are all more distant than the locations is zone i-1, where the distance associated with each storage location is the travel distance to the nearest stow station. We assume each storage location stores a pod. Similar to that in the two-class model, we are able to approximate the average travel distance for each zone by using the linear model shown in Figure 2.3 and Equation (6).

FIGURE 2.3 A linear model (Assumption A.5) for the M-class model, where β is the furthest travel distance, and J is the total number of pods in the system.

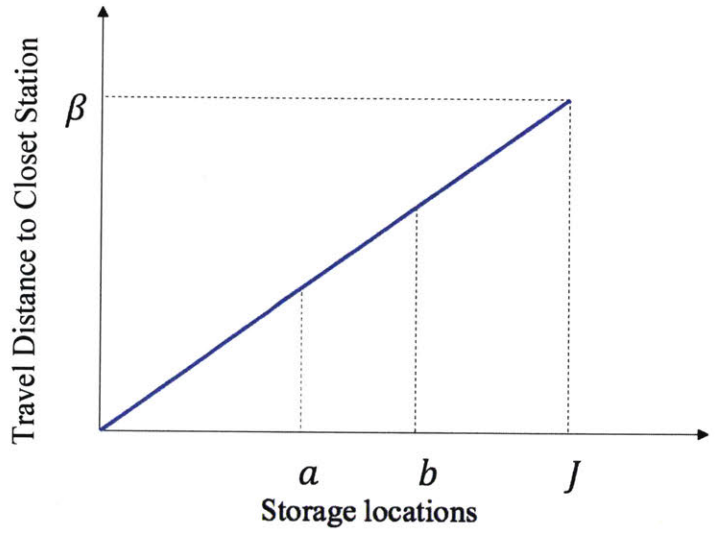

Therefore, the average travel distance to zone i can be approximated as: $\bar{d}_i = \beta(a+b)/(2J)$, where $a = J_1 + ... + J_{i-1}$, and $b = J_1 + ... + J_i$. Thus,

$$\bar{d}_i = \frac{\beta(2\sum_{j=1}^{i-1} J_j + J_i)}{2J}. \tag{22}$$

Total travel distance per hour: We now use Equation (21) and Equation (22) to estimate the total travel distance per hour for the M-class model:

$$
\begin{aligned}
T_M &= \sum_{i=1}^{M} \bar{d}_i \times N_i \\
&= \frac{\beta\lambda_S}{2k}\left(\sum_{i=1}^{M} p_i \frac{2\sum_{j=1}^{i-1} J_j + J_i}{J}\right) \\
&= \frac{\beta\lambda_S}{2k}\left(\sum_{i=1}^{M} p_i \frac{2\sum_{j=1}^{i-1} p_j\tau_j + p_i\tau_i}{\tau}\right).
\end{aligned} \tag{23}
$$

As we had $T_B = \beta\lambda_S/(2k)$, the ratio of the total stowage travel distance per hour for the M-class model compared to that of base case is:

$$
\frac{T_M}{T_B} = \sum_{i=1}^{M} p_i \frac{2\sum_{j=1}^{i-1} p_j\tau_j + p_i\tau_i}{\tau}. \tag{24}
$$

We illustrate the benefit given by Equation (24) in Table 2 for a set of numerical examples to demonstrate how the total travel distance for stowage for the M-class model decreases compared to that of the base case.

TABLE 2

Calculated Reduction in Total Travel Distance per Hour with M-class Model.

M	τ	τ_i, where $i = 1,2,...M$	p_i, where $i = 1,2,...M$	T_M/T_B
3	10	[7, 10, 12]	[0.2, 0.5, 0.3]	0.910
5	10	[5, 7, 9, 13, 17]	[0.15, 0.2, 0.25,0.3,0.1]	0.797
8	10	[3, 5, 7, 9, 11, 13, 15, 17]	[0.05, 0.1, 0.15, 0.2, 0.2, 0.15, 0.1, 0.05]	0.796

Two-Class Model with Random Stowage

In this section, we consider another case. We assume that we can categorize the units that are stowed into two classes, namely a high-velocity class and a low-velocity class. Again, we assume that we have some information on the average dwell times for the units to be stowed. However, we now assume that we do not or cannot use this information at the time of stowage. As a consequence, the stowage is random, and each pod will contain a mix of high velocity and low velocity units. Nevertheless, we can classify a pod based on its mix of high velocity and low velocity units: we will classify a pod with a high proportion of high-velocity units as a high-velocity pod, and otherwise it is a low velocity pod. As the mix of units carried by a pod changes over time, the pod classification can also change. In this section, we develop a model for analyzing this case.

At a system level, we assume there are two classes of items: high-velocity and low-velocity items. Suppose we are given the average dwell times τ_1, τ_2, where $\tau_1 < \tau_2$. The high-velocity units have an average dwell time in storage of τ_1, measured in hours; the low-velocity units have an average dwell time in storage of τ_2, measured in hours. The actual dwell time for each unit is a random variable with the given mean. We assume that there are target throughout rates, denoted as λ_1, λ_2 for the class of high-velocity units and for the class of low-velocity units, respectively. Each target throughput rate is the number of units picked per hour. We assume that this throughput rate also corresponds to the stowage rate, namely the number of units stowed per hour, based on assumption of mass balance (Assumption A.6).

The system target throughput rate, λ_s, is the sum of each class's target throughput rate, so that $\lambda_s = \lambda_1 + \lambda_2$. As we assume items are stowed randomly on the pod, the probability that an item being stowed is low velocity is then $\lambda_2/(\lambda_1 + \lambda_2)$; the probability that an item being stowed is high velocity is $\lambda_1/(\lambda_1 + \lambda_2)$.

We assume that each pod has capacity to hold C units; each pod is replenished whenever the number of units drops to $C - k$, where k is a control parameter. We assume that we can identify each unit on a pod as being either from the high-velocity or low-velocity class; but we also assume that we have no other information about the remaining dwell time for each unit. Thus, at any point of time, we know the number of high-velocity items and the number of low-velocity

items on each pod, which we can use to classify the pod as either a high or low velocity pod. After each replenishment visit to a stow station, we classify a pod as a high-velocity pod if the number of high-velocity units is greater than a threshold m; otherwise we classify the pod as a low-velocity pod. The threshold m is a control parameter. We then send the pod to different zone depending on its velocity: if it were a high-velocity pod, it would be sent to zone I, the closest locations; otherwise it would go to zone II, the furthest locations.

To analyze this policy, we use simulation of a single pod to extrapolate the system. For this extrapolation, we assume that the pods in the system operate independently. We simulate a single pod for a given specification of the inputs τ_1, τ_2, λ_1, λ_2, and the control parameters k,m. We need to specify a distribution for the unit dwell times; we assume that high (low) velocity units are exponentially distributed with average dwell time $\tau_1(\tau_2)$, respectively. For the simulation we assume that there are always units waiting to be stowed. We also assume that a high (low) velocity pod can find an open space and be stored in Zone I (II). From the simulation, we can obtain estimates of the average stay time for a high-velocity pod in Zone I, and for a low-velocity pod in zone II. We denote these as TBV_I, TBV_{II} for the 'time between visits' for zone I, and zone II. From the simulation we can also obtain estimates for the percent of time that a pod is a high-velocity pod and stored in zone I, and the percent of time the pod is a low velocity pod stored in zone II. We denote these estimates as ρ_I, ρ_{II} for zone I and II, respectively, where $\rho_I + \rho_{II} = 1$.

We can now use the estimates obtained from the simulation to characterize the performance of the policy. To do so, we assume that all pods in the system will behave as modeled by the simulated pod. We can determine both the size of each zone, which corresponds to the average number of pods in each class, and the pod arrival rate, corresponding to each storage zone. From these two parameters, we can estimate the travel distance for the system. We explain the details below.

Let J_I, J_{II}, J denote the size (in pods) of zone I, of zone II, and of the entire storage system where $J = J_I + J_{II}$. Let N_I, N_{II}, N denote the number of trips from stowage (in pods per hour) to zone I, to zone II, and to the entire storage system where $N = N_I + N_{II}$. Given the sys-

tem throughput target λ_S and the control parameter k, we can determine the average number of trips per hour to stowage:

$$N = \lambda_S / k . \tag{25}$$

As an explanation for Equation (25), we note that each stowage trip results in k units being stowed. Given the estimates ρ_I, ρ_{II} from the simulation we have the following relationships:

$$\begin{aligned} J_I &= \rho_I J, \\ J_{II} &= \rho_{II} J. \end{aligned} \tag{26}$$

As an explanation, the fraction of the total space for each type of pod should correspond to the fraction of time each pod spends in each class. Given the estimates TBV_I, TBV_{II} from the simulation, we can use Little's law to relate the number of stowage trips to each zone to the size of each zone:

$$\begin{aligned} N_I &= \frac{J_I}{TBV_I}, \\ N_{II} &= \frac{J_{II}}{TBV_{II}}. \end{aligned} \tag{27}$$

We can now substitute Equation (26) and Equation (27) into Equation (25) to obtain an estimate of J:

$$\begin{aligned} N = (N_I + N_{II}) &= \left(\frac{J_I}{TBV_I} + \frac{J_{II}}{TBV_{II}} \right) = \left(\frac{\rho_I J}{TBV_I} + \frac{\rho_{II} J}{TBV_{II}} \right) = \lambda_s / k \\ \Rightarrow J &= \frac{\lambda_s}{k \left(\frac{\rho_I}{TBV_I} + \frac{\rho_{II}}{TBV_{II}} \right)}, \end{aligned} \tag{28}$$

where we will use a simulation to obtain estimates of ρ_I, ρ_{II} and of TBV_I, TBV_{II}. The system throughput λ_S is an exogenous input and the parameter k is also an input, reflecting the frequency of stowage events.

TRAVEL DISTANCE MODEL

We now develop a model for the travel distance associated with the stowage trips.

Arrival rates from stowage to each zone: Once we have the estimates of ρ_I, ρ_{II} and of TBV_I, TBV_{II}, we can determine J from Equation (28); we can then use Equation (26) to find, J_I, J_{II}, and Equation (27) to obtain the number of trips to each class, N_I, N_{II}:

$$\begin{aligned} N_I &= \frac{J_I}{TBV_I} = \frac{\rho_I \lambda_s / TBV_I}{k\left(\frac{\rho_I}{TBV_I} + \frac{\rho_{II}}{TBV_{II}}\right)} = \frac{\lambda_S}{k} \frac{\rho_I \times TBV_{II}}{\rho_I \times TBV_{II} + \rho_{II} \times TBV_I}, \\ N_{II} &= \frac{J_{II}}{TBV_{II}} = \frac{\rho_{II} \lambda_s / TBV_{II}}{k\left(\frac{\rho_I}{TBV_I} + \frac{\rho_{II}}{TBV_{II}}\right)} = \frac{\lambda_S}{k} \frac{\rho_{II} \times TBV_I}{\rho_I \times TBV_{II} + \rho_{II} \times TBV_I}. \end{aligned} \tag{29}$$

With Equation (29), we are able to obtain that $N_I + N_{II} = (\lambda_S / k) \frac{\rho_I \times TBV_{II} + \rho_{II} \times TBV_I}{\rho_I \times TBV_{II} + \rho_{II} \times TBV_I} = \frac{\lambda_S}{k}$.

We also see that $N_I + N_{II} = \lambda_s / k = N$, agreeing with the base model that $N = \lambda_s / k$ (Equation (5)).

Average travel distance: We set zone I to be the J_I closest storage locations, and zone II to be the remaining J_{II} storage locations. With Equation (6), the average travel distance to zone I can be approximated as $\bar{d}_I = \beta J_I / (2J) = \beta \rho_I / 2$; the average travel distance to zone II can be approximated as $\bar{d}_{II} = \beta (J + J_I) / (2J) = \beta (1 + \rho_I) / 2$.

Total travel distance per hour: We can now estimate the total stowage travel distance per hour for the two-class model with random stowage as:

$$\begin{aligned} T_{2R} &= \bar{d}_I \times N_I + \bar{d}_{II} \times N_{II} \\ &= \frac{\beta \lambda_s}{2k} \left(\frac{\rho_I^2 \times TBV_{II}}{\rho_I \times TBV_{II} + \rho_{II} \times TBV_I} + \frac{(1 + \rho_I) \rho_{II} \times TBV_I}{\rho_I \times TBV_{II} + \rho_{II} \times TBV_I} \right) \\ &= \frac{\beta \lambda_s}{2k} \left(\frac{\rho_I^2 \times TBV_{II} + (1 - \rho_I^2) \times TBV_I}{\rho_I \times TBV_{II} + \rho_{II} \times TBV_I} \right). \end{aligned} \tag{30}$$

As we had $T_B = \beta \lambda_S / (2k)$, the ratio of the total stowage travel distance per hour for the Two-class model with random stowage compared to that of base case is:

$$\frac{T_{2R}}{T_B} = \frac{\rho_I^2 \times TBV_{II} + (1 - \rho_I^2) \times TBV_I}{\rho_I \times TBV_{II} + \rho_{II} \times TBV_I}. \tag{31}$$

Section 3. Simulation

The intent is to simulate a single pod to explore the benefits of velocity-based stowage policies for the semi-automated storage system.

In this section, we first verify the model of a single pod with simulation results. We then discuss and apply methods in classifying inventory for the M-class model with informed stowage. We use this simulation of a single pod to extrapolate to a storage system that is operating with a given throughput rate. For this extrapolation, we assume that the pods in the system operate independently; we assume that the dwell time for each unit in the system is exponentially distributed with an average mean, denoted by τ, measured in hours. We can then evaluate the improvement of the total stowage trip travel distance per hour for the system by varying parameters under different models, compared to the base case. We also evaluate the simulation results of the two-class model with random stowage, compared to the two-class model with informed stowage.

3.1 Verification of Model with Simulation Results

We verify the accuracy of the base case, and accuracy of the two-class model with informed stowage by simulating them in MATLAB. All models discussed in this section have input parameters including pod capacity, C, and stowage threshold, k, and average system dwell time, τ. For each model, ten samples are collected to determine the mean and 95% confidence interval (CI) for the outputs; each sample is simulated for 1000 hours of stowage events with a time increment of one minute. For the simulation, we do not need to specify the system throughput (pick) rate, λ_S, as we are verifying the model with a single pod and not evaluating the system.

Base Case

The analysis of the base case relied on an approximation given in Equation (1): the average number of units stored on each pod is approximated by $C - k/2$. We will use simulation to assess the accuracy of the model in light of this approximation. In this model, we have input parameters: $C = 100, k = 30, \tau = 10$. Ten samples are collected to determine the mean and 95% confidence interval (CI) for the outputs; each sample is simulated for 1000 hours of stowage events with a time increment of one minute.

The simulation is set up to model a single pod. The pod is initially loaded with C units of inventory. We assign a remaining dwell time to each unit of inventory on the pod; we generate each dwell time by a random draw from an exponential distribution with mean of τ hours.

The simulation operates with a fixed-time increment, with a time period of one minute. At each time increment, we deduct one minute (the time increment) from the remaining dwell time for each unit that is stored on the pod. When the remaining dwell time for a unit reaches zero, we assume that the unit gets picked and is removed from the pod. Thus, the number of units remaining on the pod is reduced by one.

Whenever the number of units on the pod reaches or drops below $C-k$ units, we have a stow action or event. We assume that the pod will travel to a stow station and that units will be stowed onto the pod to raise the number of units on the pod to C. The number of units stowed will usually be exactly k units; but occasionally, when multiple units get picked within a single time increment (one minute), then the number of units on the pod may be less than C – k units; in these cases, we will stow more than k units onto the pod, so as to bring it back to C units. For each unit that gets stowed onto the pod, we generate its dwell time, again by making a random draw from an exponential distribution with mean of τ hours. After the stow action, the process repeats.

During the simulation, we record when each stow action occurs and how many items are stowed during each stow action. With these records, we can measure the average time between visits, denoted by TBV and measured in minutes, and the average pod throughput, denoted by λ_p and measured as units per hour. Using these outputs, we calculate the total number of trips per hour, N, using Equation (4) and Equation (5), with the λ_p result; we calculated the average distance per trip, $\bar{d}$, using Equation (6) with the constant $\beta = 1$. Thus, we obtain the total stowage travel distance for the base case, T_B, using $T_B = \bar{d} \times N$ (Equation (7)).

We compare the simulation outputs with expected outputs determined by the analytical model. The details of these outputs are plotted by varying average system dwell time, τ, from 7 hours to 13 hours (Figures 3.1 – 3.3). From the results shown in Figures 3.1 – 3.3, we are able to observe that the difference between the outputs of the simulation results and those of the analytical model is small with a 95% confidence interval on the order of 1% of each measure. In addi-

tion, the difference is consistent over various average system dwell times, τ. In conclusion, the simulation results verify the accuracy of the analytical model for the base case.

FIGURE 3.1 Time Between Visits (95% CI) vs. Average System Dwell Time.

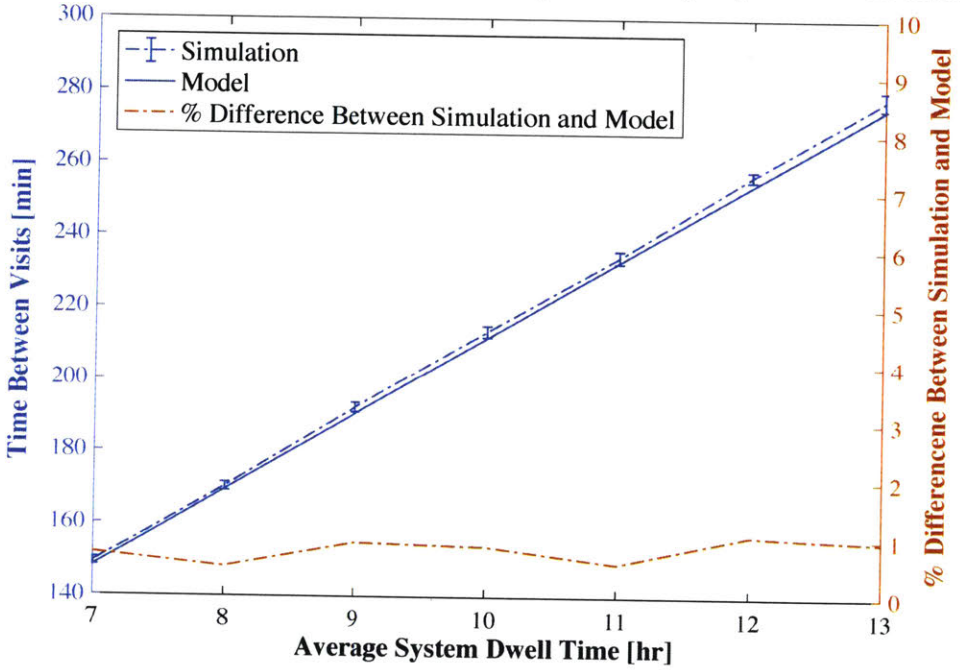

FIGURE 3.2 Pod Throughput (95% CI) vs. Average System Dwell Time.

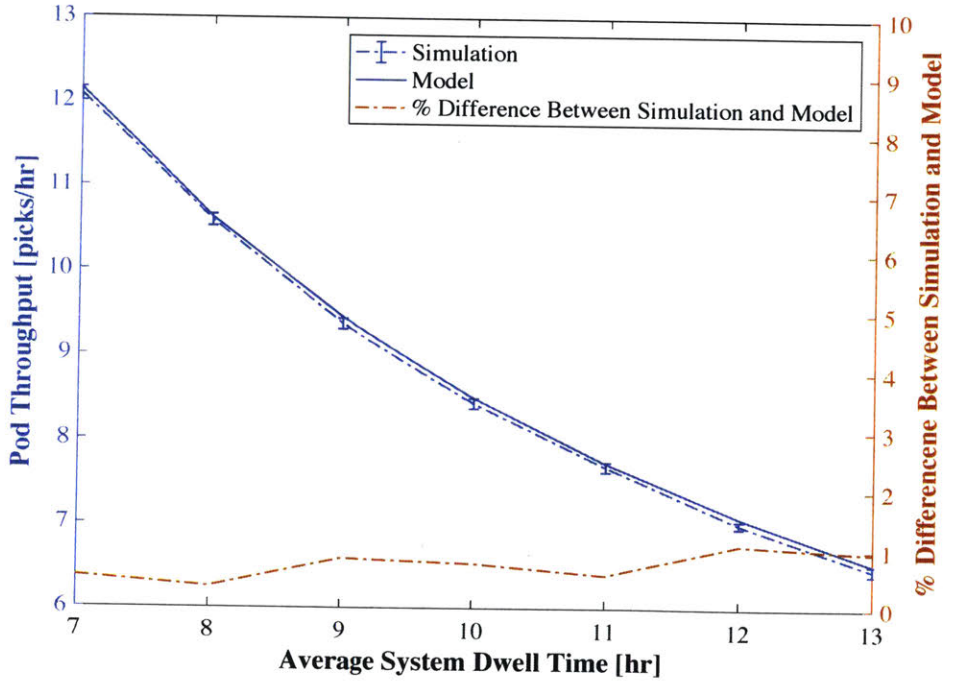

FIGURE 3.3 Number of Trips per Hour (95% CI) vs. Average System Dwell Time.

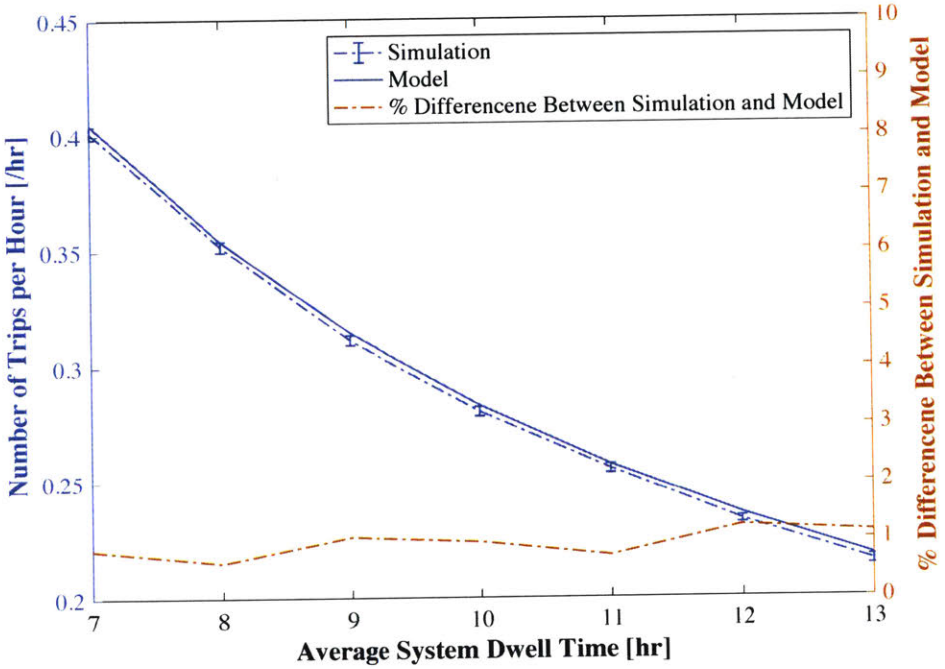

Two-Class Model with Informed Stowage

For the two-class model we need the same approximation as for the base model; we assess the accuracy of this approximation in this section with a simulation. In this model, we have input parameters: $C = 100, k = 30, \tau = 10$. In addition, we set the fraction of the arriving units that are high-velocity items, p_1, the fraction of the arriving units that are low-velocity items, p_2, the average dwell time for the high-velocity units, τ_1, and the average dwell time for the low-velocity units, τ_2,. For the base case example we assume that the input parameters are $p_1 = 0.2$, $p_2 = 0.8$, $\tau_1/\tau_2 = 5$. The relationship among p_1, p_2, τ_1, τ_2 satisfies Equation (8). We conduct ten simulation samples where we simulate 1000 hours of storage events in each sample. We then can use the outputs to determine the mean and 95% confidence interval (CI) for the measures of interest.

The simulation setup is similar with that of the base case. For the base case, we conduct one simulation of a single pod, as all pods should behave the same under random stowage. For the two-class model, we need two simulations: one for simulating a single pod that holds only

high-velocity units, and the other to simulate a single pod that holds only low velocity units. Otherwise, the logic of each simulation is the same as for the base case.

For the M-class model the setup of the simulation is the same, but now we need to conduct M simulations, one for each class of units and pods.

We compare the simulation outputs with expected outputs determined by the analytical model. The details of these outputs are plotted by varying average system dwell time, τ, from 7 hours to 13 hours (Figures 3.4 – 3.9). From the results shown in Figures 3.4 – 3.9, we are able to see that the difference between the outputs of the simulation result and those of the analytical model is significantly small. In addition, the difference is consistent over various average system dwell times, τ. In conclusion, the analytical model is verified with simulation results.

FIGURE 3.4 High-Velocity Pod: Time Between Visits (95% CI) vs. Avg. System Dwell Time.

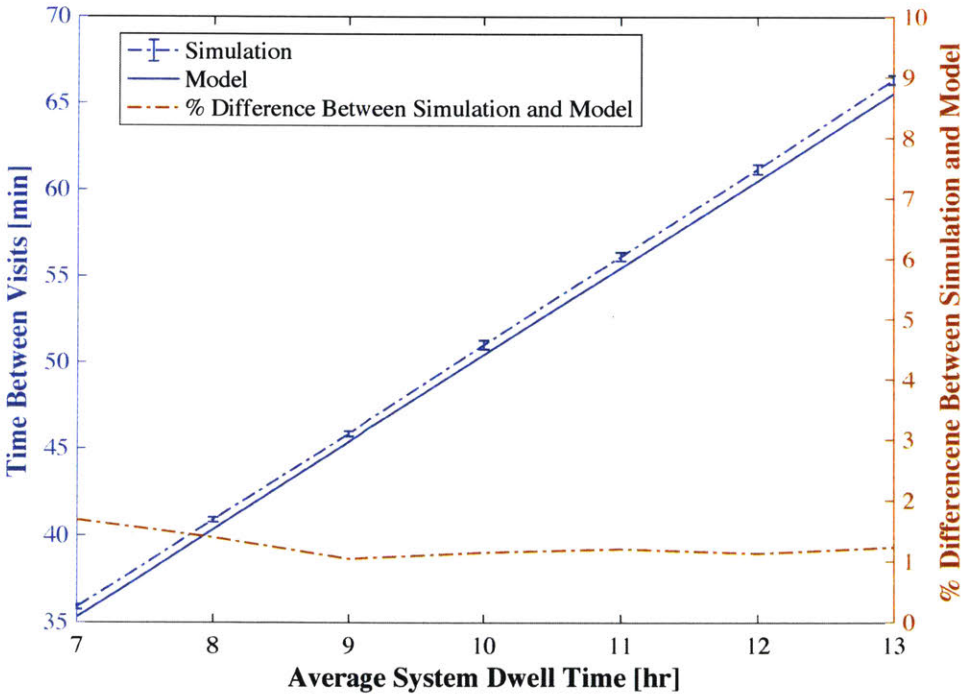

FIGURE 3.5 Low-Velocity Pod: Time Between Visits (95% CI) vs. Avg. System Dwell Time.

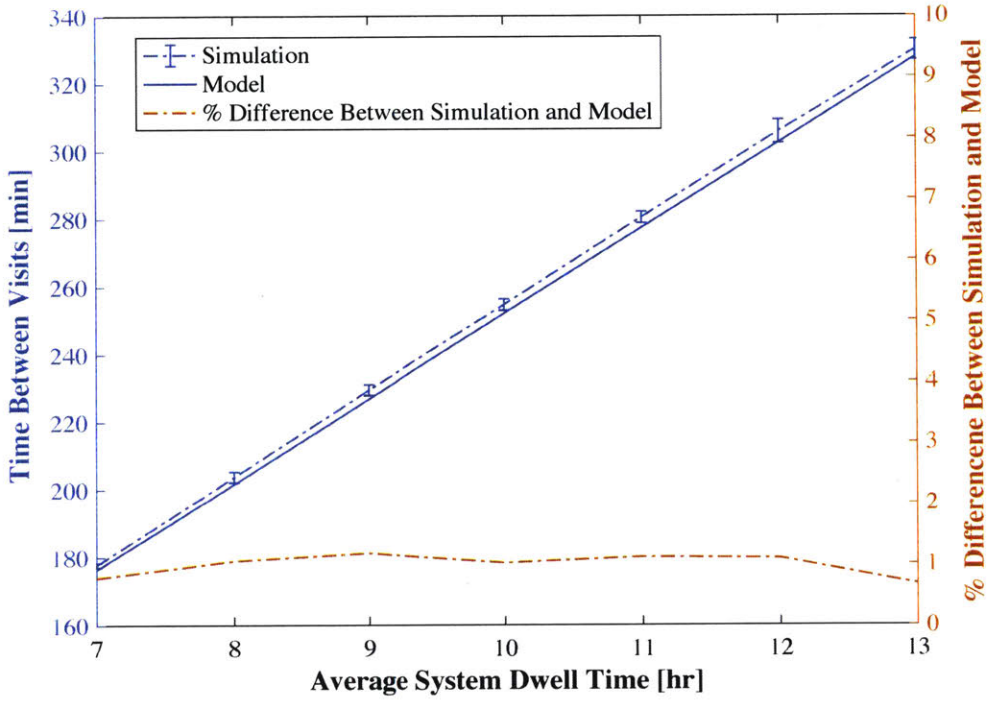

FIGURE 3.6 High-Velocity Pod: Pod Throughput (95% CI) vs. Avg. System Dwell Time.

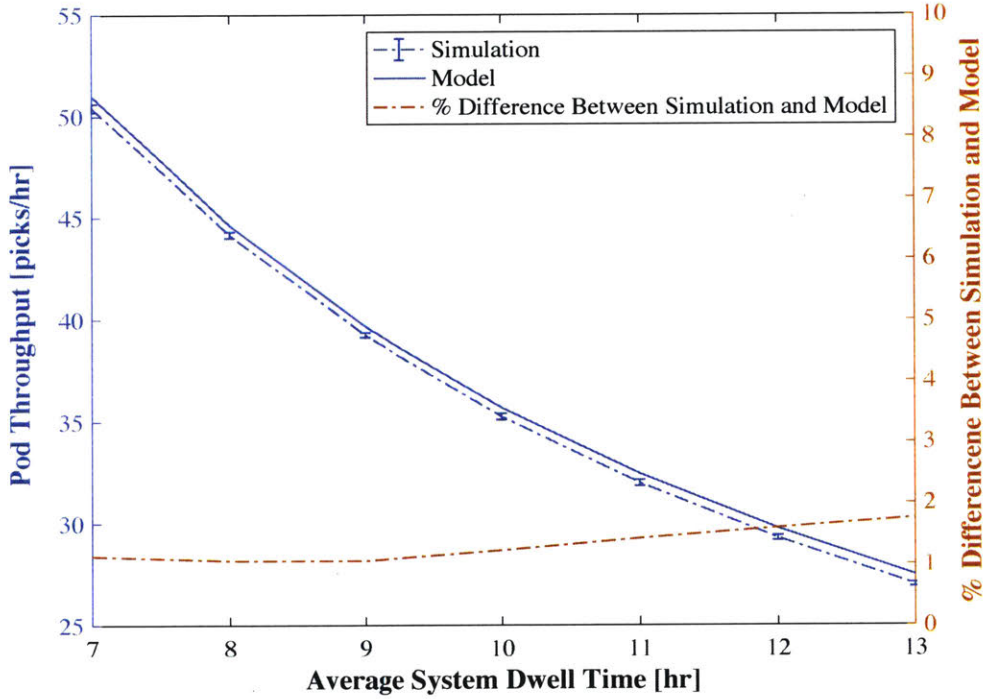

FIGURE 3.7 Low-Velocity Pod: Pod Throughput (95% CI) vs. Avg. System Dwell Time.

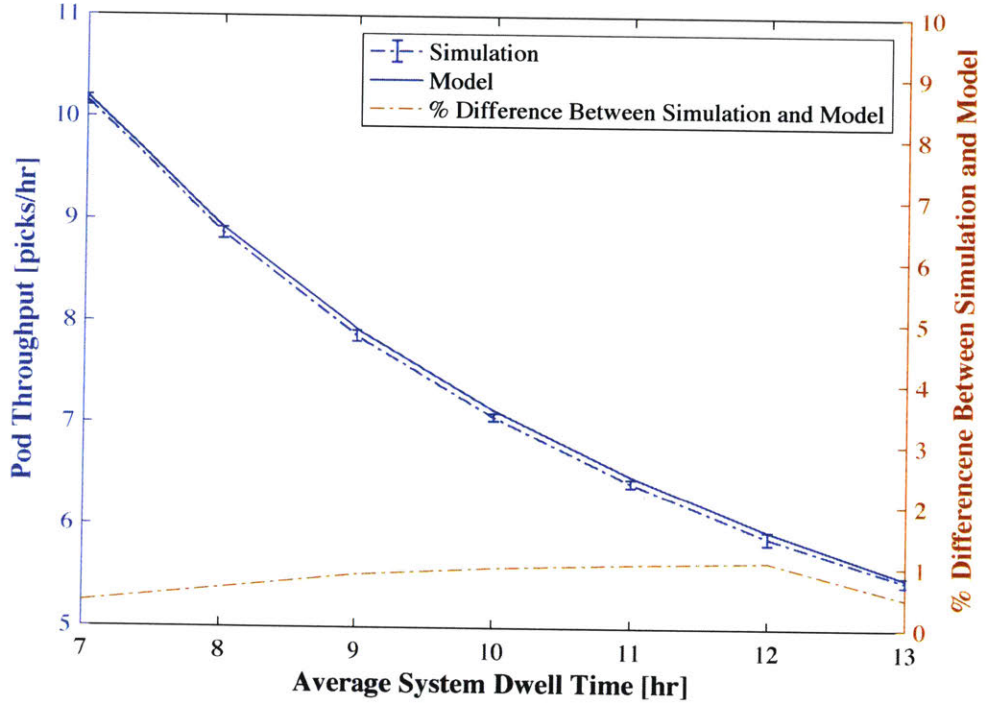

FIGURE 3.8 High-Velocity Pod: Number of Trips (95% CI) vs. Avg. System Dwell Time.

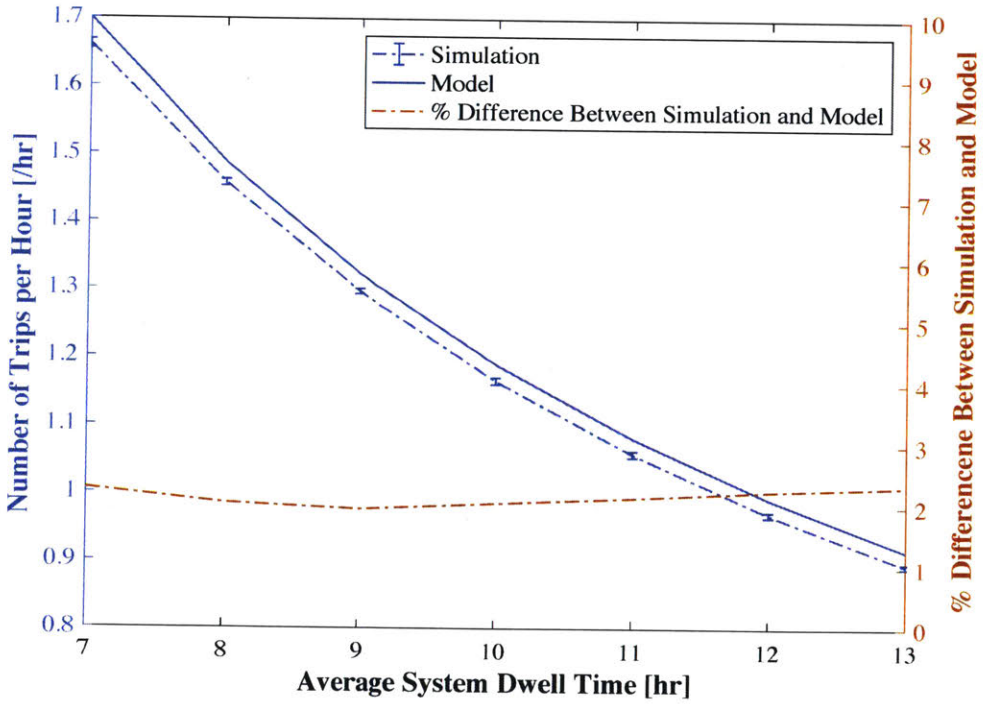

FIGURE 3.9 Low-Velocity Pod: Number of Trips (95% CI) vs. Average System Dwell Time.

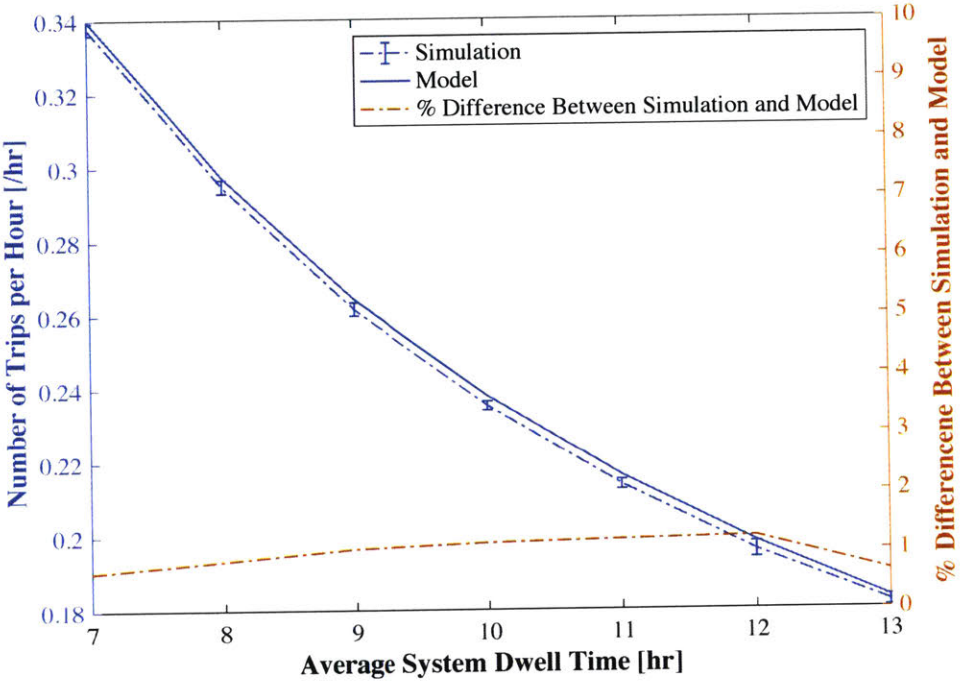

3.2 Classification of inventory for M-class model with Informed Stowage

We wish to explore the benefits of the two-class and M-class model, as they depend on the nature of the item demand seen by the storage system. We expect that the more skewed the demand distribution is, the greater will be the benefits from a velocity-based stowage policy. We will use a continuous model for the demand distribution across the assortment of items in the storage system, and partition the inventory assortment into multiple segments, or classes.

We assume that we have a very large number of items or skus that are stowed into the system. We assume that each item has a demand (or pick) rate and an average system inventory level; the demand rate is the rate at which units are picked from the system, as well as the rate at which units are stowed into the system by Assumption A.6. We define λ_i as the demand rate for item i, in units picked or stowed per hour (Assumption A.6), and Q_i as the average inventory level in the storage system for item i, in units. We assume the demand rate for each item is known, and we are able to index the items in decreasing order of the demand rate, in which

$\lambda_i \geq \lambda_{i+1}$. The average dwell time for each unit of item i in the storage system, τ_i, can be determined by Little's Law: $\tau_i = Q_i/\lambda_i$, in hours.

We will use a continuous model of the assortment of items stored in the system. For the continuous model, we assume a very large number of items, and we assume that we can index these items on a continuum from 0 to 1, where $i \in (0,1)$. We assume the items are ordered by their demand rates such that $\lambda(i) \geq \lambda(j), \forall i < j$ where $\lambda(i)$ denotes the demand rate at the i^{th} percentile of the assortment of items. We define a cumulative demand function, denoted by $G(i)$, to equal the cumulative demand rate for all items $j \in (0,i)$. We model this cumulative demand function in the following form, similar to the "*ABC*" curve:

$$G(i) = \lambda_S i^s \text{ for } 0 < s < 1, \tag{32}$$

where $G(i)$ is the amount of demand accounted for the i^{th} percentile highest demanded items, λ_S is the demand or throughput rate for the system, and parameter s controls the shape of the cumulative demand function (as shown in Figure 3.10). In Figure 3.10, for instance, the 20/60 rule indicates that 20% of the items in the system accounts for 60% of the total demand; The parameter s can be obtained by solving $G(i=0.2)/\lambda_S = 0.6 = 0.2^s$. This form has been previously used in Haurman et al. (1976). Here, $G(i)$ is an increasing concave function.

FIGURE 3.10 $G(i)$ is the amount of demand accounted for vs. i^{th} percentile highest demanded items, where λ_S is normalized as 1.

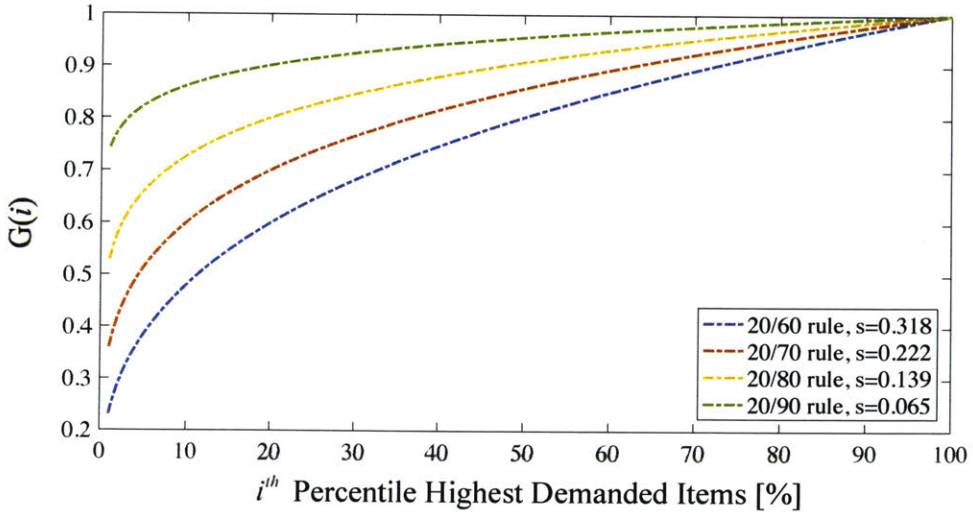

By differentiating $G(i)$, we obtain the demand rate at the i^{th} percentile as

$$\lambda(i) = \lambda_S s i^{s-1}, \tag{33}$$

where $s, i \in (0,1)$. We now assume that the average inventory for item i in the storage system, Q_i, is proportional to the ρ^{th} root of the demand rate for $\rho \geq 1$. That is, we assume that:

$$Q(i) = \eta \sqrt[\rho]{\lambda(i)} = \eta \sqrt[\rho]{\lambda_S s i^{s-1}}, \tag{34}$$

where η is the proportionality constant. Therefore, with Equation (34), we can express the average dwell time for item i as:

$$\tau(i) = Q(i) \Big/ \lambda(i) = \eta \sqrt[\rho]{\lambda(i)} \Big/ \lambda(i) = \eta \Big/ (\lambda(i))^{1-1/\rho}. \tag{35}$$

For instance, assuming $\rho = 2$, with Equation (33), the average dwell time for item i is

$$\tau(i) = \eta \Big/ \sqrt{\lambda(i)} = \eta \Big/ \sqrt{\lambda_S s i^{s-1}}. \tag{36}$$

In the following we will assume that $\rho = 2$. In this way, with Equation(36), assuming $\rho = 2$, the average dwell time for all the items in the storage system, τ, can be expressed as

$$\tau = \int_{i=0}^{1} \frac{\tau(i)\lambda(i)}{\lambda_S} di = \int_{i=0}^{1} \frac{\eta \sqrt{\lambda(i)}}{\lambda_S} di. \tag{37}$$

With Equation (33), Equation (37) becomes

$$\begin{aligned} \tau &= \eta \int_{i=0}^{1} \sqrt{\frac{s i^{s-1}}{\lambda_S}} di \\ &= \eta \sqrt{s/\lambda_S} \frac{2}{s+1} i^{s+1/2} \Big|_{i=0}^{i=1} \\ &= \frac{2\eta \sqrt{s/\lambda_S}}{s+1}. \end{aligned} \tag{38}$$

We wish to use this model to generate numerical examples for which we can evaluate the benefits from the velocity-based stowage policies. In order to specify the numerical examples for

the M-class Model, we will assume that we are able to segment the items into classes based on their demand rates. Let us use $(j,k)=\{i \mid j<i\le k\}$ to denote a set of items; that is, (j,k) denotes the items indexed from the j^{th} to k^{th} percentile highest demand. Let $p(j,k)$ denote the fraction of demand attributable to this set,

$$p(j,k)=\int_{i=j}^{k}\frac{\lambda(i)}{\lambda_S}di=k^s-j^s. \tag{39}$$

Let $\tau(j,k)$ denote the demand-weighted dwell time for this set of items. We can express this as follows:

$$\tau(j,k)=\int_{i=j}^{k}\tau(i)\frac{\lambda(i)}{\lambda_S}di=\frac{2\eta\sqrt{s/\lambda_S}}{s+1}\left(k^{\frac{s+1}{2}}-j^{\frac{s+1}{2}}\right). \tag{40}$$

From Equation (38), we observe that $\eta=\tau(s+1)/(2\sqrt{s/\lambda_S})$. We can then re-write Equation (40) as:

$$\tau(j,k)=\tau(j,k)=\frac{2\eta\sqrt{s/\lambda_S}}{s+1}\left(k^{\frac{s+1}{2}}-j^{\frac{s+1}{2}}\right)=\tau\left(k^{\frac{s+1}{2}}-j^{\frac{s+1}{2}}\right). \tag{41}$$

Assume Class Z contains the items indexed from the j^{th} to k^{th} percentile highest demand. In order to obtain the average dwell time for a class Z, τ_Z, we need to normalize Equation (41) by dividing by the fraction of demand attributable to Class Z, p_Z, and Equation (39)

$$\tau_Z=\frac{\tau(j,k)}{p(j,k)}=\tau\frac{\left(k^{\frac{s+1}{2}}-j^{\frac{s+1}{2}}\right)}{k^s-j^s}. \tag{42}$$

With Equation (42), we are able to solve for the average dwell time for each class by varying the partitioning points and given average system dwell times. Therefore we are able to use Equation (24), presented in the M-class model, to obtain the ratio of T_M/T_B, which represents the reduction in total stowage travel distance for the M-class model, compared to the base case.

We give an example of classifying the inventory for the three-class model (M=3) in Table 3. We assume that we can index the items on a continuum of $(0,1)$. We set Class 1 to be the first five percent of the t item, namely the items in the interval $(0,0.05]$. We set Class 2 to be the

next 15% of the items, namely items from the interval (0.05,0.20], and Class 3 is the remaining items from (0.20,1). We set the average system dwell time, τ, as 10 hours. We present the example with values of parameter s from the 20/60, 20/70, 20/80, and 20/90 rules. We use the example results $p_1, p_2, p_3, \tau_1, \tau_2, \tau_3$ to approximate T_M/T_B using Equation (24).

TABLE 3

Three-class Model with Informed Stowage Example: Classification of inventory and T_3/T_B Result.

ABC Curve*	Parameter s	p_1	p_2	p_3	τ_1	τ_2	τ_3	T_3/T_B
20/60 Rule	0.318	0.39	0.21	0.40	3.60	9.70	16.32	0.87
20/70 Rule	0.222	0.51	0.19	0.30	3.12	11.53	20.83	0.76
20/80 Rule	0.139	0.66	0.14	0.20	2.75	15.58	29.94	0.59
20/90 Rule	0.065	0.82	0.08	0.10	2.47	28.56	57.95	0.35

* The 20/60 rule indicates that 20% of the items in the system accounts for 60% of the total demand; et cetera. The parameter s can be obtained by solving $G(i=0.2)/\lambda_S = 0.6 = 0.2^s$.

3.3 Simulation Results for M-class Model with Informed Stowage (*M*=2 & 3)

In this section, the ratio of T_M/T_B is obtained from evaluating the M-class model with informed stowage for $M=2\&3$, using the approach to classify inventory that is demonstrated in the previous section. We simulate the base case and M-class model with informed stowage (*M*=2 & 3) to obtain we the simulated T_M/T_B. We will use the simulation to assess the accuracy of the analytical approximation by using Equation (24). All models discussed in this section have input parameters including pod capacity, C, and stowage threshold, k, and average system dwell time, τ, and system throughput (pick) rate, λ_S. For each model, ten samples are collected to determine the mean and 95% confidence interval (CI) for the outputs; each sample is simulated with 1000 hours. We simulate the models under the 20/60, 20/70, 20/80, and 20/90 rules.

Simulation Setup

The simulation setup is similar to the one shown in Section 3.1. We simulate the base case for comparison, and M-class model with informed stowage (*M*=2 & 3). The models in this section have input parameters: $C=100, k=30, \tau=10, \lambda_S=1000$. We use the classification approach demonstrated in Section 3.2 to obtain the fraction of incoming items as Class i, p_i, and

the Class i average dwell time, τ_i, for $i = 1,2...M$, by inputting the percentage of Class i items with the given τ. The percentage of items for each class is varied to demonstrate its impact on the ratio of T_M/T_B, which represents the reduction in the total stowage travel distance for the M-class model, compared to the base case.

Two-class Model (M=2)

The simulation results for the two-class model are shown in Figure 3.11. The percentage of items as Class 1 varies from 1% to 50% to show its impact on T_2/T_B from both the simulation and the analytical model using Equation (15). The difference between the simulation results and expected output from the analytical model is significantly small, which further verifies the model with simulation results.

From Figure 3.11, we observe that by increasing the percentage of items as Class 1, T_2/T_B decreases to a minimum, and then starts to increase. In addition, the result shows that the model underestimates the simulation result more when the demand is more skewed, where 20% of items account for more of the total demand. This result could be because a higher percentage of Class 1 items increases the high-velocity pod travel frequency in the system, resulting in less heterogeneity for the system. Thus, the system benefits less from the two-class model with informed stowage in reduction in total travel by having a high percentage of Class 1 items.

We can use the analytical model to solve for the percentage of Class 1 items to minimize T_2, where the system could benefit the most in reducing total stowage travel distance from the two-class model with informed stowage. Let us use $(0,a] = \{i \mid 0 < i \le a\}$ to denote the set of items in Class 1, where $i \in (0,1)$. By differentiating Equation (15) with a partitioning point of Class 1 items, x, and using Equation (39) and Equation (42), we are able obtain

$$\frac{d(T_2/T_B)}{dx} = \frac{\delta(1-p_1+p_1\frac{\tau_1}{\tau})}{dx}$$
$$= \frac{d\left(1-(k^s-j^s)+(k^s-j^s)\frac{k^{s+1/2}-j^{s+1/2}}{k^s-j^s}\right)}{dx}, k=x, j=0 \qquad (43)$$
$$= \frac{d\left(1-x^s+x^{s+1/2}\right)}{dx}$$
$$= -sx^{s-1}+\frac{s+1}{2}x^{s-1/2}.$$

Then, let Equation (43) equal zero to solve for the partitioning point, $x = a_{\min}$, for the analytical minimum of T_2/T_B, which could be input into (15) to obtain the analytical minimum of T_2/T_B, denoted as $T_2/T_B(a_{\min})$. The calculated $a_{\min}$ and $T_2/T_B(a_{\min})$ for each rule are shown in Table 4. Even though the two-class model with informed stowage is able to provide maximum benefit in reducing total stowage travel distance around $a_{\min}$, the model performs well with a relatively wide range around the optimal partitioning point for the model under the 20/60, 20/70, and 20/80 rules, where the 20/60 rule is likely the real life scenario.

FIGURE 3.11 T_2/T_B by simulation (95% CI) and model vs. Percentage of items as Class 1.

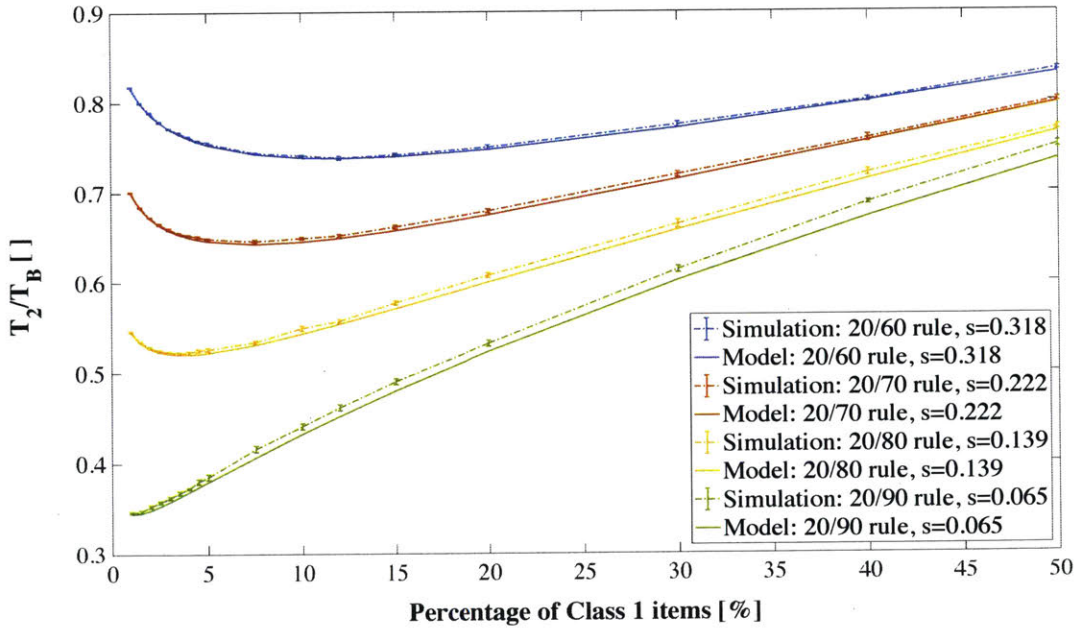

TABLE 4

Two-class Model with Informed Stowage: Analytical Result for Maximum Reduction in Total Travel Distance per Hour.

ABC Curve*	Parameter s	$a_{\min}$	$T_2/T_B(a_{\min})$
20/60 Rule	0.318	0.118	0.73
20/70 Rule	0.222	0.074	0.64
20/80 Rule	0.139	0.038	0.52
20/90 Rule	0.065	0.011	0.34

* The 20/60 rule indicates that 20% of the items in the system accounts for 60% of the total demand; et cetera. The parameter s can be obtained by solving $G(i=0.2)/\lambda_S = 0.6 = 0.2^s$.

Three-class Model (M=3)

The evaluation for the three-class model is shown in Figures 3.12 – 3.17. The percentage of items as Class 1 is varied from 10% to 30%, and the percentage of items as Class 2 is varied from 20% to 40% to show their impact on T_3/T_B from both the simulation and the analytical model using Equation (24).

Figures 3.12 – 3.14 show the result of T_3/T_B by holding the percentage of Class 1 items the same, and varying the percentage of Class 2 items. We observe that varying the percentage of Class 2 items with the same percentage of Class 1 items does not have a significant impact on the result of T_3/T_B. However, we can still observe a trend similar to that shown in the two-class model: the model underestimates the simulation results when the demand is more skewed, where 20% of items account for more of the total demand. Figures 3.15 – 3.17 show the result of T_3/T_B by holding the percentage of Class 2 items the same, and varying the percentage of Class 1 items. We observe an increasing trend of T_3/T_B when the percentage of Class 1 items increases. When the demand is more skewed, we also observe that the trend becomes steeper, and the model underestimates the simulation result more.

As we observe that the analytical model is a reliable approximation to the simulation, we are able to find the recommended partitioning for each class using a two-stage optimization. We first vary the percentage of Class 1 items within a boundary, and with each percentage of Class 1, we vary the percentage of Class 2 within another boundary. We set the boundary of each class as: Class 1 ranges from 0.01 to 40%, Class 2 ranges from 1 to 50%, and Class 3 is the rest. We

evaluate the analytical result by incrementing Class 1 and Class 2 with a size of 0.01%. From the enumeration of the range of combinations, we are able to find the partitioning of the assortment that minimizes T_3/T_B. These results are summarized in Table 5.

The three-class model with informed stowage performs well with a relatively wide range around the optimal partitioning point for the model: under the 20/60 rule, by varying percentage of items as Class 1 within 1 – 9%, and Class 2 within 12 – 46%, we can obtain most T_3/T_B results less than 0.70; under the 20/70 rule, by varying percentage of items as Class 1 within 1 – 4%, and Class 2 within 10 – 38%, we can obtain most T_3/T_B results less than 0.59; under the 20/80 rule, by varying percentage of items as Class 1 within 1 – 2%, and Class 2 within 6 – 35%, we can obtain most T_3/T_B results less than 0.46; under the 20/90 rule, by varying percentage of items as Class 1 within 1%, and Class 2 within 2 – 26%, we can obtain most T_3/T_B results less than 0.28.

In conclusion, the three-class model with informed stowage provides greater but diminishing reduction in the total stowage travel distance, compared to the two-class model with informed stowage. The reduction in total stowage travel distance is primarily determined by the percentage of items as Class 1, and is less sensitive to the percentage of items as Class 2.

FIGURE 3.12 Class 1 = 10%: T_3/T_B by simulation (95% CI) & model vs. Pct. of Class 2 items

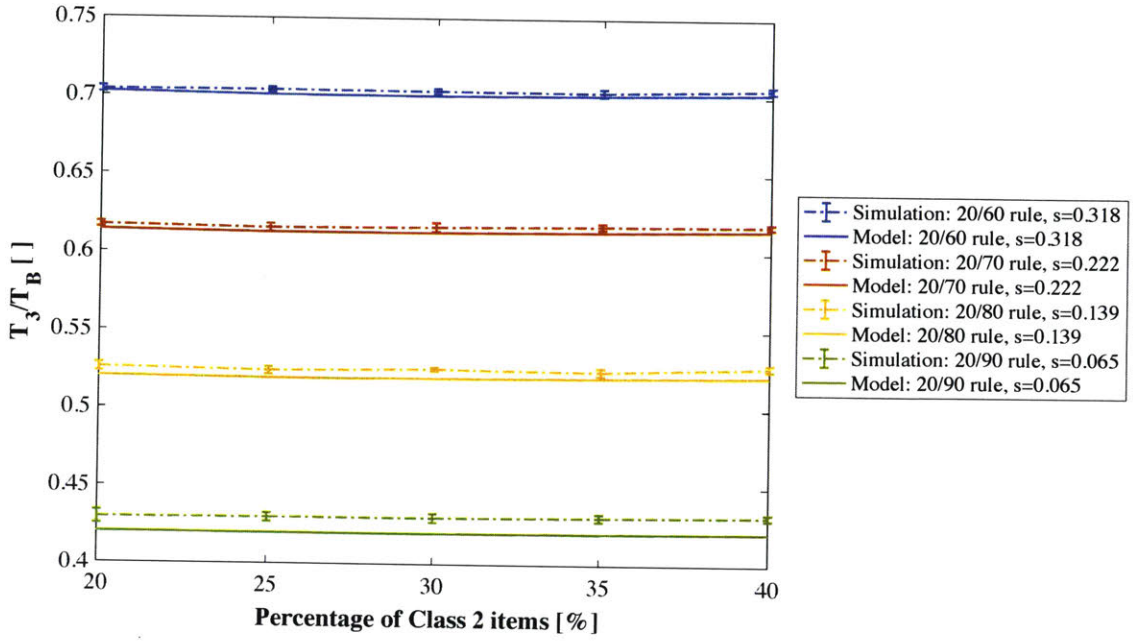

FIGURE 3.13 Class 1 = 20%: T_3/T_B by simulation (95% CI) & model vs. Pct. of Class 2 items

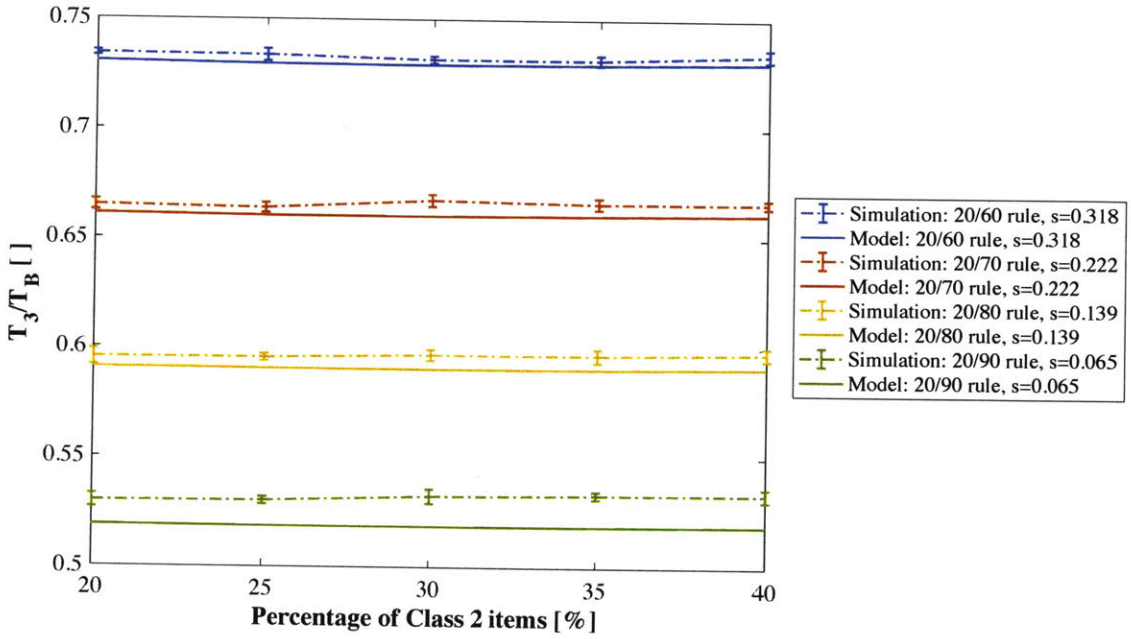

FIGURE 3.14 Class 1 = 30%: T_3/T_B by simulation (95% CI) & model vs. Pct. of Class 2 items

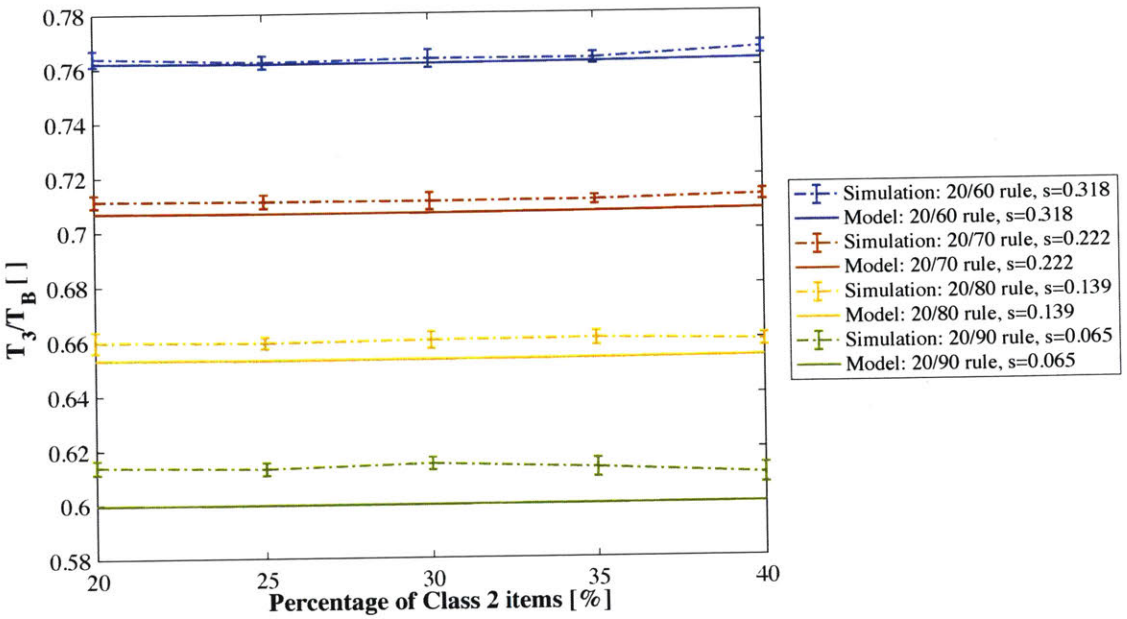

FIGURE 3.15 Class 2 = 20%: T_3/T_B by simulation (95% CI) & model vs. Pct. of Class 1 items

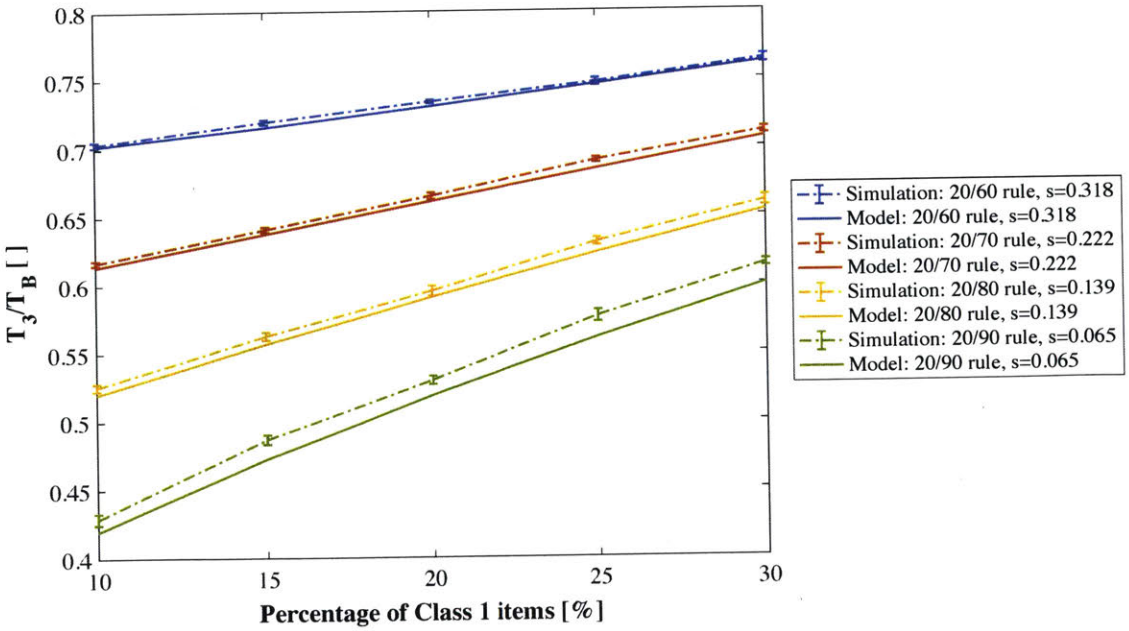

FIGURE 3.16 Class 2 = 30%: T_3/T_B by simulation (95% CI) & model vs. Pct. of Class 1 items

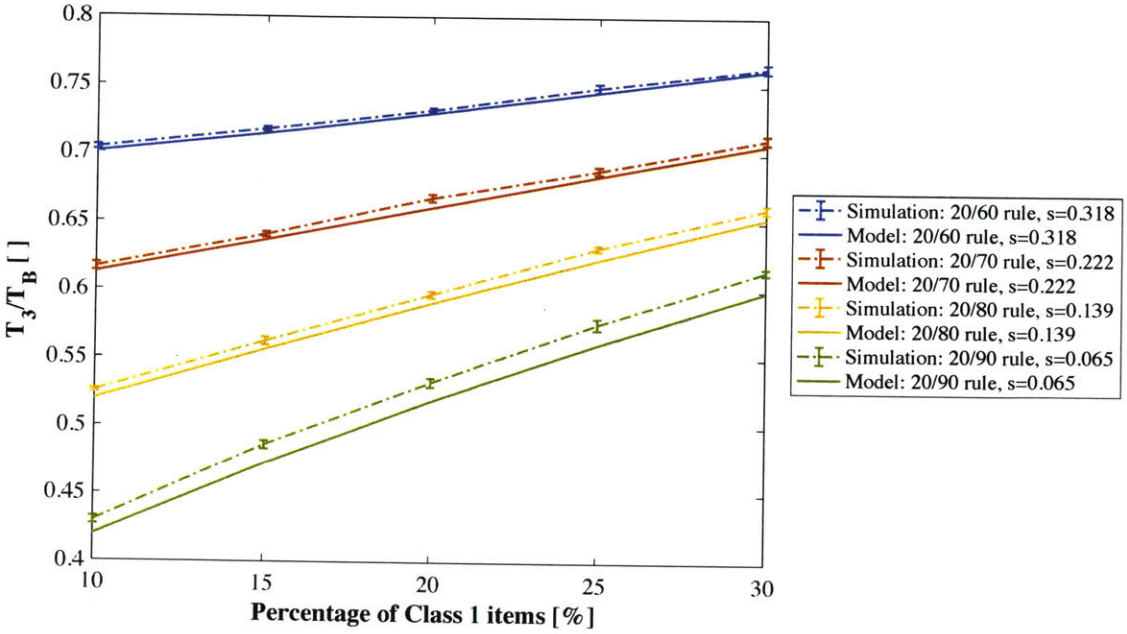

FIGURE 3.17 Class 2 = 40%: T_3/T_B by simulation and model vs. Pct. of Class 1 items

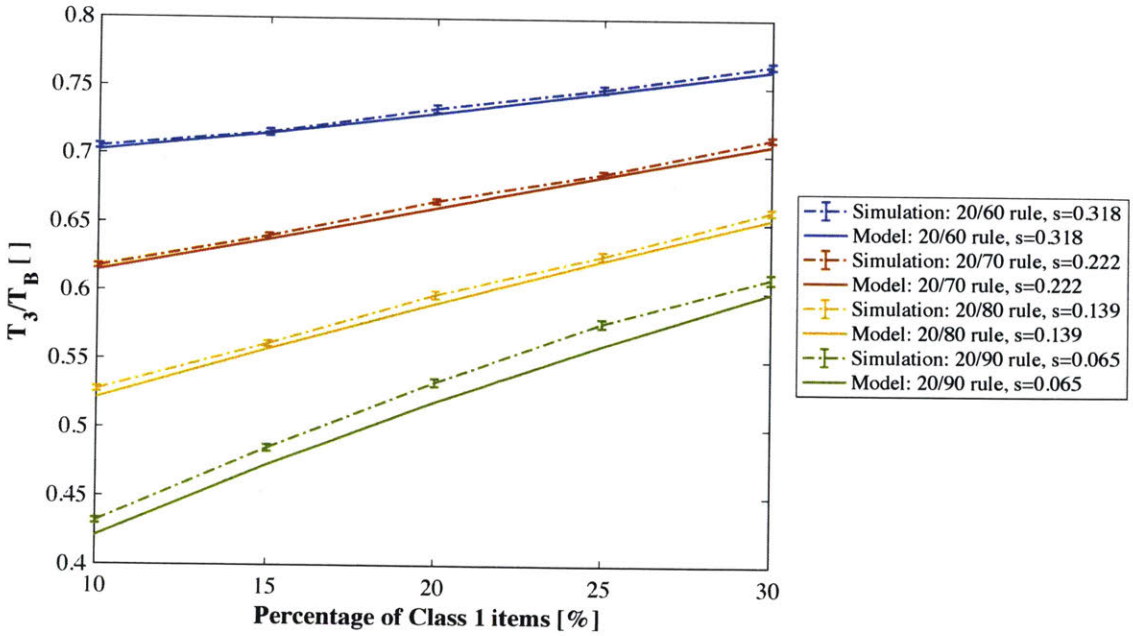

TABLE 5

Three-class Model with Informed Stowage: Analytical and Simulated Result (95% CI) for Maximum Reduction in Total Travel Distance per Hour by Two-stage Optimization.

ABC Curve*	Parameter s	Class 1 items %	Class 2 items %	Class 3 items %	Analytical T_3/T_B	Simulated T_3/T_B	Simulated T_3/T_B 95% CI
20/60 Rule	0.318	3.4	25.3	71.3	0.69	0.69	0.688 – 0.692
20/70 Rule	0.222	1.7	19.7	78.6	0.58	0.58	0.581 – 0.585
20/80 Rule	0.139	0.6	15.3	84.0	0.45	0.45	0.447 – 0.451
20/90 Rule	0.065	0.1	9.2	90.7	0.27	0.27	0.268 – 0.270

* The 20/60 rule indicates that 20% of the items in the system accounts for 60% of the total demand; et cetera. The parameter s can be obtained by solving $G(i=0.2)/\lambda_S = 0.6 = 0.2^s$.

3.4 Simulation Results for Two-class Model with Random Stowage

In this section, the ratio of T_{2R}/T_B is obtained from simulating the two-class model with random stowage (using Equation (30)) and compared with the ratio of T_2/T_B obtained from simulating two-class model with informed stowage. We simulate the base case for comparison. In this model, we have input parameters including pod capacity, C, and stowage threshold, k, and average system dwell time, τ, and system throughput (pick) rate, λ_S. For each model, ten samples are collected to determine the mean and 95% confidence interval (CI) for the outputs; each sample is simulated with 1000 hours. We simulate the models under the 20/60, 20/70, 20/80, and 20/90 rules.

Simulation Setup

For the two-class model with random stowage, the simulation setup is the same as that of the base case. However, in addition to recording when each stow action occurs and how many items are stowed for each stow action, we also record the status of the pod after the stow action. After each stow action, we classify a pod as a high-velocity pod if the number of high-velocity units is greater than a threshold m; otherwise we classify the pod as a low-velocity pod. With these records, we use the simulation to obtain performance estimates for the high-velocity (low-velocity) pod: the fraction of time that a pod is a high-velocity pod (low-velocity pod) and stored in zone I (II), denote by $\rho_I(\rho_{II})$; the time between visits, denoted by $TVB_I(TVB_{II})$ and measured

in minutes; the number of trips each pod makes per hour, denoted by $1/TBV_I (1/TBV_{II})$. We use these high-velocity (low-velocity) pod outputs to calculate: the total number of trips per hour, $N_1(N_2)$, using Equation (26), (27) and (28), with the $1/TBV_I (1/TBV_{II})$, $\rho_I(\rho_{II})$ results and input parameter λ_S; the average distance per trip, $\bar{d}_1(\bar{d}_2)$, using Equation (6) with the constant $\beta = 1$. Thus, we obtain the total stowage travel distance for the two-class model with random stowage, T_{2R}, using $T_{2R} = \bar{d}_I \times N_I + \bar{d}_{II} \times N_{II}$ (Equation (30)).

In this model, we have input parameters: $C = 100, k = 30, \tau = 10, \lambda_S = 1000$. The threshold, m, is varied from 1% to 50% (normalized with pod capacity C) to demonstrate the improvement of the total stowage trip travel distance per hour for two-class model with random stowage, compared to the base case. The simulation results are shown in Figure 3.18 and 3.19. In Figure 3.18, we observe that the two-class model with random stowage is able to decrease the total stowage travel distance but not as much as informed stowage does (shown in Figure 3.11). By varying the threshold, m, we can observe a minimum under each rule by using the two-class model with random stowage. As shown in the Section 3.3, the fulfillment systems are able to gain more benefits from the two-class model with informed stowage when the demand is more skewed. However, for the two-class model with random stowage, the fulfillment systems are able to gain more benefits when the demand is less skewed. Figure 3.19 shows how the heterogeneity across the pods is affected by the threshold, m. We observe that the fraction of time as high-velocity pod, ρ_I, decreases to 0 or increases to 1 when m, is too low or too high. The fraction of time as high-velocity pod, ρ_I, is most sensitive to the change in the threshold, m, when ranging around 20% - 35%.

In Table 6, we record the threshold, $m_{\min}$, that maximizes the reduction in total travel distance by random stowage, $T_{2R}/T_B(m_{\min})$. The portion of time as high-velocity pod with threshold $m_{\min}$, denoted as $\rho_I(m_{\min})$, is around 0.4 - 0.5, which validates that greater reduction in total travel distance can be achieved under a greater heterogeneity across the pods. In Table 6, we also compared the reduction in total travel distance by random stowage to that by informed stowage. For the two-class model with informed stowage we set for comparison, the simulation setup is the same as the one in Section 3.3; the input parameters are $C = 100, k = 30, \tau = 10, \lambda_S = 1000$; and

as we previously assumed that we can index the items on a continuum of (0,1), we set Class 1 to be (0,0.05], Class 2 to be (0.05,1). We use the classification approach demonstrated in Section 3.2 to obtain the fraction of incoming items as high-velocity (low-velocity) items, $p_1(p_2)$ and high-velocity (low-velocity) items average dwell time, $\tau_1(\tau_2)$ by inputting the percentage of Class i items and the given τ. We obtain results of T_2 under the 20/60, 20/70, 20/80, and 20/90 rules. The corresponding fraction of incoming items as high-velocity (low-velocity) items, p_1, p_2, are:

$$p_1 = 0.39, p_2 = 0.61 \text{ under the 20/60 rule;}$$

$$p_1 = 0.51, p_2 = 0.49 \text{ under the 20/70 rule;}$$

$$p_1 = 0.66, p_2 = 0.34 \text{ under the 20/80 rule;}$$

$$p_1 = 0.82, p_2 = 0.18 \text{ under the 20/69 rule.}$$

We calculate the fraction of the maximum possible improvement with $(1-T_{2R}/T_B)/(1-T_2/T_B)$. We observe that random stowage is able to achieve a higher fraction of the maximum possible improvement when the demand is less skewed.

FIGURE 3.18 Simulation Results: T_{2R}/T_B vs. Threshold, *m*, for High-velocity Pod

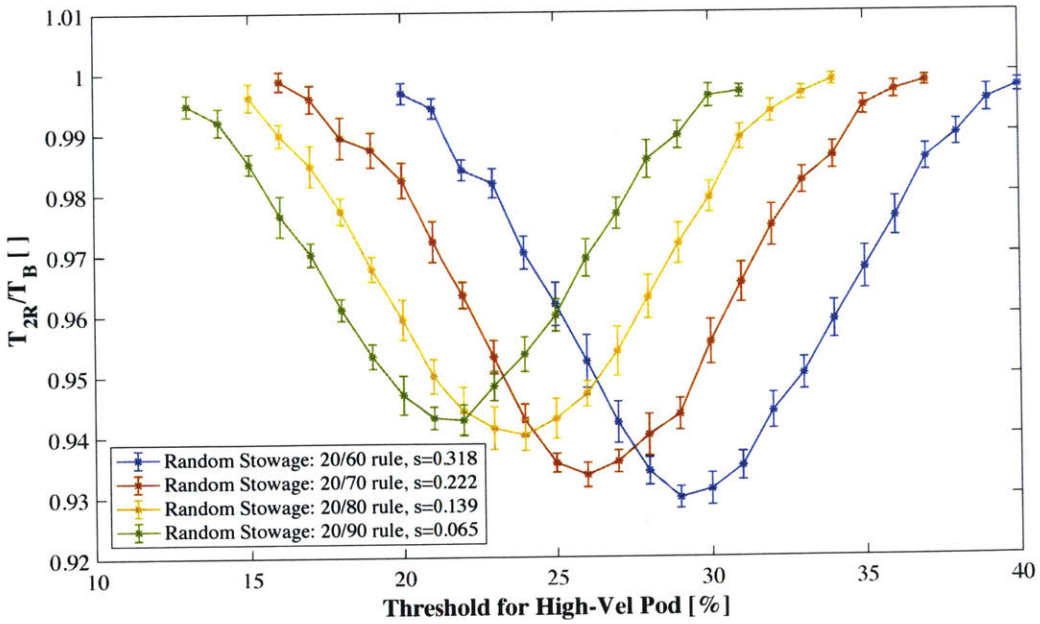

FIGURE 3.19 Simulation Results: Fraction of Time as High-velocity Pod, ρ_I vs. Threshold, m, for High-velocity Pod

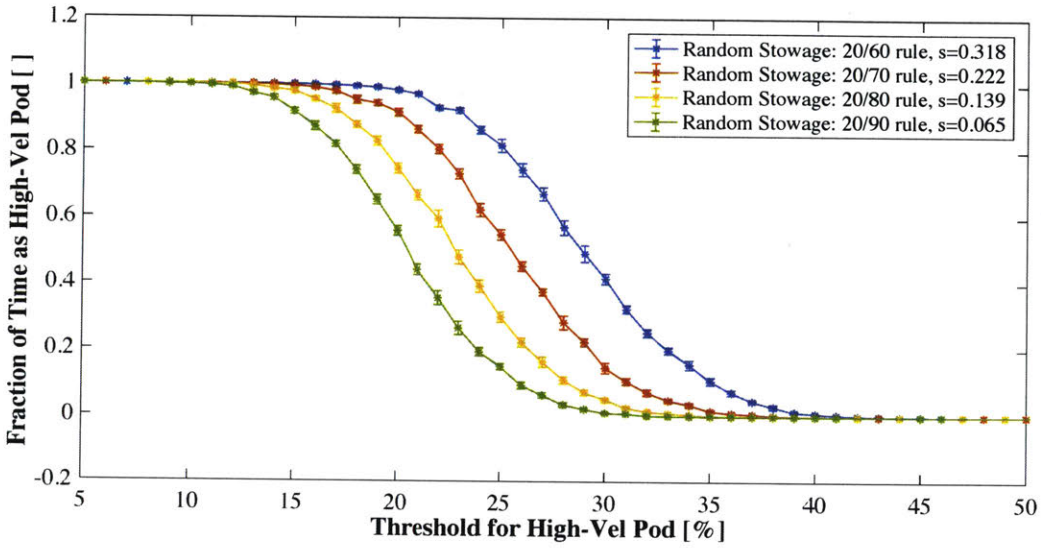

TABLE 6

Two-class Model with Random Stowage: Simulation Results for Maximum Reduction in Total Travel Distance per Hour

ABC Curve*	Parameter s	$m_{\min}$	$\rho_I(m_{\min})$	$T_{2R}/T_B(m_{\min})$	Fraction of Max. Possible Improvement by Informed Stowage
20/60 Rule	0.318	29%	0.48	0.93	28.7%
20/70 Rule	0.222	26%	0.37	0.93	19.0%
20/80 Rule	0.139	24%	0.48	0.94	12.9%
20/90 Rule	0.065	22%	0.44	0.94	9.5%

* The 20/60 rule indicates that 20% of the items in the system accounts for 60% of the total demand; et cetera. The parameter s can be obtained by solving $G(i=0.2)/\lambda_S = 0.6 = 0.2^s$.

Section 4. Conclusion

In this thesis, we model three types of stowage policies: two-class with informed stowage, M-class with informed stowage, and two-class with random stowage. We consider random stowage policy as our base case, in which units are not stowed based on their velocity. We use both simulation and analytical results to show the impact on reducing the total travel distance compared to that of the base case.

We assume that we can categorize the units to be stowed into classes for the two-class and M-class model with informed stowage, and we derive the equations for the reduction in total travel distance under each model compared to that of the base case. We also analyze the case of two-class model with random stowage, and develop an equation for calculating the total travel distance; we use simulation to estimate the parameters needed in this evaluation equation.

Using simulation, we verify the accuracy of the model. We simulate the behavior of a single pod, and then argue that we can extrapolate the results from the single pod to a storage system that is operating with a given throughput rate. From the two-class and three-class model with informed stowage, we observe that the fulfillment system is able to benefit more when the demand is more skewed. We are able to see a greater but diminishing reduction in total system travel distance under the three-class model compared to that of the two-class model with informed stowage. We also evaluate the benefits of the two-class model with random stowage from the simulation, compared with the two-class model with informed stowage. From the two-class with random stowage, we observe that the fulfillment system is able to benefit more when the demand is less skewed and when the system is more heterogeneous.

References

Ali, F. (2018). *U.S. e-commerce sales grow 16.0% in 2017 | Digital Commerce 360.* [online] Digital Commerce 360. Available at: https://www.digitalcommerce360.com/article/us-ecommerce-sales/ [Accessed 22 May 2018].

Bozer, Y.A. and Aldarondo, F.J., 2018. A simulation-based comparison of two goods-to-person order picking systems in an online retail setting. *International Journal of Production Research*, pp.1-21.

De Koster, R., Le-Duc, T. and Roodbergen, K.J., 2007. Design and control of warehouse order picking: A literature review. *European journal of operational research*, *182*(2), pp.481-501.

Enright, J. and Wurman, P.R., 2011, August. Optimization and Coordinated Autonomy in Mobile Fulfillment Systems. In *Automated action planning for autonomous mobile robots* (pp. 33-38).

Gagliardi, J.P., Renaud, J. and Ruiz, A., 2012. Models for automated storage and retrieval systems: a literature review. *International Journal of Production Research*, *50*(24), pp.7110-7125.

Graves, S.C., Hausman, W.H. and Schwarz, L.B., 1977. Storage-retrieval interleaving in automatic warehousing systems. *Management science*, *23*(9), pp.935-945.

Handfield, R., Straube, F., Pfohl, H.C. and Wieland, A., 2013. Embracing global logistics complexity to drive market advantage. *DVV Media Group GmbH, BVL International.*

Hausman, W.H., Schwarz, L.B. and Graves, S.C., 1976. Optimal storage assignment in automatic warehousing systems. *Management science*, *22*(6), pp.629-638.

Lamballais, T., Roy, D. and De Koster, M.B.M., 2017a. Estimating performance in a robotic mobile fulfillment system. *European Journal of Operational Research*, *256*(3), pp.976-990.

Lamballais, T., Roy, D. and De Koster, M.B.M., 2017b. Inventory Allocation in Robotic Mobile Fulfillment Systems.

Merschformann, M., Lamballais, T., de Koster, R. and Suhl, L., 2018. Decision Rules for Robotic Mobile Fulfillment Systems. *arXiv preprint arXiv:1801.06703.*

Nigam, S., Roy, D., Koster, R.D. and Adan, I., 2014. Analysis of class-based storage strategies for the mobile shelf-based order pick system.

Roodbergen, K.J. and Vis, I.F., 2009. A survey of literature on automated storage and retrieval systems. *European journal of operational research*, *194*(2), pp.343-362.

Wurman, P.R., D'Andrea, R. and Mountz, M., 2008. Coordinating hundreds of cooperative, autonomous vehicles in warehouses. *AI magazine*, *29*(1), p.9.

Yuan, R., 2016. *Velocity-based storage and stowage decisions in a semi-automated fulfillment system* (Doctoral dissertation, Massachusetts Institute of Technology).

Yuan, R., Cezik, T. and Graves, S.C., 2018a. Velocity-Based Storage Assignment in Semi-Automated Storage Systems.

Yuan, R., Cezik, T. and Graves, S.C., 2018b. Stowage decisions in multi-zone storage systems. *International Journal of Production Research*, *56*(1-2), pp.333-343.

Zou, B., Gong, Y., Xu, X. and Yuan, Z., 2017. Assignment rules in robotic mobile fulfilment systems for online retailers. *International Journal of Production Research*, *55*(20), pp.6175-6192.